



Efficient Conformance Checking using Alignment Computation with Tandem Repeats

Daniel Reißner^a, Abel Armas-Cervantes^a, Marcello La Rosa^a

^a *University of Melbourne, Australia*

Abstract

Conformance checking encompasses a body of process mining techniques which aim to find and describe the differences between a process model capturing the expected process behavior and a corresponding event log recording the observed behavior. Alignments are an established technique to compute the distance between a trace in the event log and the closest execution trace of a corresponding process model. Given a cost function, an alignment is optimal when it contains the least number of mismatches between a log trace and a model trace. Determining optimal alignments, however, is computationally expensive, especially in light of the growing size and complexity of event logs from practice, which can easily exceed one million events with traces of several hundred activities. A common limitation of existing alignment techniques is the inability to exploit repetitions in the log. By exploiting a specific form of sequential pattern in traces, namely *tandem repeats*, we propose a novel technique that uses pre- and post-processing steps to compress the length of a trace and recomputes the alignment cost while guaranteeing that the cost result never under-approximates the optimal cost. In an extensive empirical evaluation with 50 real-life model-log pairs and against five state-of-the-art alignment techniques, we show that the proposed compression approach systematically outperforms the baselines by up to an order of magnitude in the presence of traces with repetitions, and that the cost over-approximation, when it occurs, is negligible.

Keywords: Process mining, Conformance checking, Alignment, Tandem repeat, Petri net

1. Introduction

Business processes are the backbone of modern organizations [1]. Processes such as order-to-cash or procure-to-pay are executed hundreds of times in sales and retail organizations, as claims handling or loan origination processes are core to the success of financial companies such as insurances and banks. These processes are supported by one or more enterprise systems. For example, sales processes are typically supported by an enterprise resource planning system while claims handling processes are supported by claims management systems. These systems maintain detailed execution traces of the business processes they support, in the form of so-called *event logs*. An event log contains sequences of events (called *traces*) that are performed within a given process case, e.g. for a given order or claim application. In turn, each event refers to the execution of a particular process activity, such as “Check purchase order” or “Assess credit risk” and is timestamped based on the activity completion time.

Email addresses: dreissner@student.unimelb.edu.au (Daniel Reißner), abel.armas@unimelb.edu.au (Abel Armas-Cervantes), marcello.larosa@unimelb.edu.au (Marcello La Rosa)

Process mining techniques aim to extract insights from event logs, in order to assist organizations in their operational excellence or digital transformation programs [2, 1]. Conformance checking is a specific family of process mining techniques whose goal is to identify and describe the differences between an event log and a corresponding process model [2, 1]. While the event log captures the observed business process behavior (the as-is process), the process model used as input by conformance checking techniques captures the expected behavior of the process (the to-be or prescriptive process).

A common approach for conformance checking is by computing *alignments* between traces in the log and execution traces that may be generated by the process model. In this context, a trace alignment is a data structure that describes the differences between a log trace and a possible model trace. These differences are captured as a sequence of moves, including *synchronous moves* (moving forward both in the log trace and in the model trace) and *asynchronous moves* (moving forward either only in the log trace or only in the model trace). A desirable feature of a conformance checking technique is that it should identify a minimal (yet complete) set of behavioral differences. In trace alignments this means that the computed alignments should have a minimal length, or more generally, a *minimal cost*. Existing techniques that fulfill these properties, e.g. [3, 4], exhibit scalability limitations in the context of large and complex real-life logs. In fact, the sheer number of events in a log and the length of each trace are rapidly increasing, as logging mechanisms of modern enterprise systems become more fine-grained, as well as business processes become more complex to comply with more stringent regulations. For example, the BPI Challenge 2018 [5], one of the logs used in the evaluation of this paper, features around 2.5M events with traces up to 3K events in length. State-of-the-art alignment techniques are worst-case exponential in time on the length of the log traces and the size of the process model. This lack of scalability hampers the use of such techniques in interactive settings as well as in use cases where it is necessary to apply conformance checking repeatedly, for example in the context of automated process discovery [6], where several candidate models need to be compared by computing their conformance with respect to a given log.

This paper starts from the observation that activities are often repeated within the same process case, e.g. the amendment of a purchase request may be performed several times in the context of a procure-to-pay process, due to errors in the request. In the case of the BPI Challenge 2018 log, nearly half of the 3,000 activities in the longest trace are in fact repeated. When computing alignments, the events corresponding to these repeated activities are aligned with the same loop structure in the process model. Based on this, we use *tandem repeats* [7, 8], a type of sequential pattern, to encode repeated sequences of events in the log and collapse them to two occurrences per sequence, effectively reducing the number of times the repeated sequence needs to be aligned with a loop structure in the process model. When computing alignments, we use an adjusted cost function to prioritize repeatable sequences in the process model for the collapsed sequences of events in the log. Later, we extend these collapsed sequences to form alignments that fully represent again the events in the original log traces, and form a valid path through the process model. Collapsing such sequences also allows us to reduce the number of unique traces in the log, since two different traces may differ only in the number of occurrences of a given sequence of events, so when reduced, these two traces may map to the same unique trace. We can then use a binary search to find if the reduction of different sequence of repeated events leads to the same reduced alignment for a unique trace. If that is the case, we can reuse these alignments for several original traces, leading to a further improvement in computational performance.

We apply this technique to a specific class of Petri nets, namely free-choice, concurrency-free Petri nets with unique activity labels. Free choice Petri nets have been shown to be a versatile class of Petri nets as they map directly to BPMN models with core elements, which are widely used in practice. Next, we show how the technique can be integrated into a decomposition framework for alignment computation, to relax the concurrency-free requirement.

We implemented our technique as an open-source tool as part of the Apromore software ecosystem. Using this tool, we extensively evaluated the efficiency and accuracy of the technique via a battery of 50 real-life model-log pairs, against five baseline approaches for alignment computation.

The rest of this paper is organized as followed. Section 2 discusses existing conformance checking and string compression techniques. Next, Section 3 introduces preliminary definitions and notations related to Automata-based conformance checking, alignments and tandem repeats. Section 4 then presents our

technique while Section 5 discusses the results of the empirical evaluation. Finally, Section 6 summarizes the contributions and discusses avenues for future work.

2. Related Work

In this section we review different approaches for alignment computation in conformance checking, and techniques for string compression.

2.1. Alignment approaches

Conformance checking in process mining aims at relating the behavior captured in a process model with the behavior observed in an event log. In this article, we specifically focus on identifying behavior observed in the log that is disallowed by the model (a.k.a. unfitting behavior). One central artifact in process mining for measuring unfitting behavior are *trace alignments*. Hereafter, we introduce the concept of alignments and then review existing techniques for computing trace alignments.

Trace alignment. Trace alignments, first introduced in [3, 9], relate each trace in the event log to its closest execution in the process model in terms of its Levenshtein distance. In this context, an alignment of two traces is a sequence of *moves* (or *edit operations*) that describes how two cursors can move from the start of the two traces to their end. In a nutshell, there are two types of edit operations. A *match* operation indicates that the next event is the same in both traces. Hence, both cursors can move forward synchronously by one position along both traces. Meanwhile, a *hide* operation (deletion of an element in one of the traces) indicates that the next events are different in each of the two traces. Alternatively, one of the cursors has reached the end of its trace while the other has not reached its end yet. Hence, one cursor advances along its traces by one position while the other cursor does not move. An alignment is optimal if it contains a minimal number of hide operations. Given that a process model can contain a possibly infinite set of traces due to loop structures, several traces can have alignments with minimal distance for the same trace of the event log. In this article, we focus on techniques that compute only one minimal distance alignment for each trace of the event log.

In the following, we first review approaches that compute (exact) trace alignments with minimal distance. These techniques have a worst-case exponential time complexity in terms of the length of the input trace and the size of the process model. Hence, several approaches have been proposed to compute trace alignments with *approximate* cost or that deploy *divide-and-conquer* strategies. These latter two categories of approaches are reviewed afterwards.

Exact techniques. The idea of computing alignments between a process model (captured as a Petri net) and an event log was developed in Adriansyah et al. [3, 9]. This proposal maps each trace in the log into a (perfectly sequential) Petri net. It then constructs a synchronous Petri nets as a product out of the model and the trace net. Finally, it applies an A^* algorithm to find the shortest path through the synchronous net which represents an optimal alignment. Van Dongen [4] extends Adriansyah et al.’s approach by strengthening the underlying heuristic function. This latter approach was shown to outperform [3, 9] on an artificial dataset and a handful of real-life event log-model pairs. In the evaluation reported later in this article, we use both [3, 9] and [4] as baselines.

In previous work [10], we translate both the event log and the process model into automata structures. Then, we use an A^* algorithm to compute minimal distance trace alignments by bi-simulating each trace of the event log on both automata structures allowing for asynchronous moves, i.e. the edit operations. This approach utilizes the structure of the automata to define prefix and suffix memoization tables in order to avoid re-computing partial alignments for common trace prefixes and suffixes. This approach was shown to outperform [3, 9] on some real-life and synthetic datasets. We also retain this technique as a baseline approach for the evaluation section.

De Leoni et al. [11] translate the trace alignment problem into an automated planning problem. Their argument is that a standard automated planner provides a more standardized implementation and more configuration possibilities from the route planning domain. Depending on the planner implementation, this

approach can either provide optimal or approximate solutions. In their evaluation, De Leoni et al. showed that their approach can outperform [3] only on very large process models. Subsequently, [4] empirically showed that trace alignment techniques based on the A* heuristics outperform the technique of De Leoni et al. in the general case. Accordingly, in this article we do not retain the technique by De Leoni et al. as a baseline.

In the above approaches, each trace is aligned to the process model separately. An alternative approach, explored in [12], is to align the entire log against the process model, rather than aligning each trace separately. Concretely, this approach transforms both the event log and the process model into *event structures* [13]. It then computes a synchronized product of these two event structures. Based on this product, a set of natural-language statements are derived, which characterize all behavioral relations between activities captured in the model but not observed in the log and vice-versa. The emphasis of this *behavioral alignment* is on the completeness and interpretability of the set of difference statements that it produces. As shown in [12], the technique is less scalable than that of [3, 9], in part due to the complexity of the algorithms used to derive an event structure from a process model. Since the emphasis of the present article is on scalability, we do not retain [12] as a baseline. On the other hand, the technique proposed in this article computes as output the same data structure as [12] – a so-called Partially Synchronised Product (PSP). Hence, the output of the technique proposed in this article can be used to derive the same natural-language difference statements produced by the approach in [12].

Approximate techniques. In order to cope with the inherent complexity of the problem of computing optimal alignments, several authors have proposed algorithms to compute approximate alignments. We review the main approaches below. *Sequential alignments* [14] is one such approximate approach. This approach implements an incremental method to calculate alignments. It uses an ILP program to find the cheapest edit operations for a fixed number of steps (e.g. three events) taking into account an estimate of the cost of the remaining alignment. The approach then recursively extends the found solution with another fixed number of steps until a full alignment is computed. We do not use this approach as a baseline in our empirical evaluation since its core idea was used in the extended marking equation alignment approach presented in [4], which derives optimal alignments and exhibits better performance than Sequential Alignments. In other words, [4] subsumes [14].

Another approximate alignment approach, namely *Alignments of Large Instances* or ALI [15], finds an initial candidate alignment using a replay technique and improves it using a local search algorithm until no further improvements can be found. This approach has shown promising results in terms of scalability when compared to the exact trace alignment approaches presented in [3, 9, 4]. Accordingly, we use this technique as a further baseline in our evaluation.

Another approach is the *evolutionary approximate alignments* [16]. It encodes the computation of alignments as a genetic algorithm. Tailored crossover and mutation operators are applied to an initial population of model mismatches to derive a set of alignments for each trace. In this article, we focus on computing one alignment per trace (not all possible alignments) and thus we do not consider approaches like [16] as baselines in our evaluation. Approaches that compute all-optimal alignments are slower than those that compute a single optimal alignment per trace, and hence the comparison would be unfair.

Bauer et al. [17] propose to use *trace sampling* to approximately measure the amount of unfitting behavior between an event log and a process model. The authors use a measure of trace similarity in order to identify subsets of traces that may be left out without substantially affecting the resulting measure of unfitting behavior. This approach does not address the problem of computing trace alignments, but rather the problem of (approximately) measuring the level of fitness between an event log and a process model. In this respect, trace sampling is orthogonal to the contribution of this article. Trace sampling can be applied as a pre-processing step prior to any other trace alignment approach, including the techniques presented in this article.

Last, Burattin et al. [18] propose an approximate approach to find alignments in an online setting. In this approach, the input is an event stream instead of an event log. Since traces are not complete in such an online setting, the approach computes alignments of trace prefixes and estimates the remaining cost of a possible suffix. The emphasis is on the quality of the alignments made for trace prefixes, and as such, this

approach is not directly comparable to trace alignment techniques that take full traces as input.

Divide-and-conquer approaches. In divide-and-conquer approaches, the process model is split into smaller parts to speed up the computation of alignments by reducing the size of the search space. Van der aalst et al. [19] propose a set of criteria for a valid decomposition of a process model in the context of conformance checking. One decomposition approach that fulfills these criteria is the *single-entry-single-exit* (SESE) process model decomposition approach. Munoz-Gama et al. [20] present a trace alignment approach based on SESE decomposition. The idea is to compute an alignment between each SESE fragment of a process model and the event log projected onto this model fragment. An advantage of this approach is that it can pinpoint mismatches to specific fragments of the process model. However, it does not compute alignments at the level of the full traces of the log – it only produces partial alignments between a given trace and each SESE fragment. A similar approach is presented in [21].

Verbeek et al. [22] present an extension of the approach in [20], which merges the partial trace alignments produced for each SESE fragment in order to obtain a full alignment of a trace. This latter approach sometimes computes optimal alignments, but other times it produces so-called *pseudo-alignments* – i.e., alignments that correspond to a trace in the log but not necessarily to a trace in the process model. In this article, the goal is to produce actual alignments (not pseudo-alignments). Therefore, we do not retain [22] as a baseline.

Song et al. [23] present another approach for recomposing partial alignments, which does not produce pseudo-alignments. Specifically, if the merging algorithm in [22] cannot recompose two partial alignments into an optimal combined alignment, the algorithm merges the corresponding model fragments and re-computes a partial alignment for the merged fragment. This procedure is repeated until the re-composition yields an optimal alignment. In the worst case, this may require computing an alignment between the trace and the entire process model. A limitation of [23] is that it requires a manual model decomposition of the process model as input. The goal of the present article is to compute alignments between a log and a process model automatically, and hence we do not retain [23] as a baseline.

Last, in [24] we extend the Automata-based approach from [10] to a decomposition-recomposition approach based on *S-Components*. This approach first decomposes the input process model into concurrency-free sub models, i.e. its S-Components, based on the place invariants of the process model. Then it applies the Automata-based approach to each pair of S-Component and a sub-log derived by trace projection. Next, the approach recomposes the decomposed alignments of each S-Component to form proper alignments for full traces of the event log. This approach was shown to outperform both [3, 9] and [4] on process models with concurrency on a set of real-life log-model pairs. Therefore, we keep the S-Components approach as a baseline in the evaluation section.

2.2. String compression techniques

The technique presented in this article relies on a particular type of sequential pattern mining, namely *tandem repeats*, and specifically on string compression techniques to detect and collapse repeated sequences of events, so as to reduce the length of the traces in a log. In the rest of this section we review different types of string compression techniques, and the types of repetitive patterns that can be compressed. Last, we review the usage of string compression techniques in process mining.

Lossless vs. loss-prone compression approaches. String or text compression techniques can be broken down into two families of approaches: *dictionary based-approaches* and *statistical approaches* [25]. Dictionary-based approaches aim at achieving a *lossless* representation of the input data by recording all reduced versions of repetitive patterns in the data source in a dictionary to be able to later reconstruct an exact representation of the original data. Statistical approaches on the other hand rely on statistical models such as alphabet or probability distributions to compress the input data. This type of approaches can achieve a better degree of compression, but can only reconstruct an approximate representation of the original data, i.e. the compression is *prone to the loss of information*. As such, this latter approach is more applicable when a small loss of information is tolerable and the amount of information is very large, e.g. in the field of image compression. In the context of trace alignment, this is not suitable because any loss of information

may result in further (spurious) differences between the log and the model. Hence, our focus is on lossless compression techniques.

Dictionary based approaches can be further sub-divided into approaches that implicitly represent compressed sequences as tuples, i.e. approaches based on “Lempel Ziv 77” [26], or explicitly record compressions in a dictionary, i.e. approaches based on “Lempel Ziv 78” [27]. The former approaches aims at identifying the longest match of repetitive patterns in a sliding window and compresses the repeated pattern with a tuple consisting of an offset to the previous repetition, the length of the pattern and the first symbol after the pattern. Several approaches improved on this idea by reducing the information of the tuple or by improving the identification of repetitions [28].

Approaches based on Lempel Ziv 78 build up a dictionary for compressed repetitive sequences such that each compressed pattern is linked to an index of its extended form in the dictionary. When the input source is very large, the dictionary will grow extensively as well lead to a lower compression rate. Several approaches tackled this issue by using different types of dictionaries, for example with static length [29] or over a rolling window [30]. Both types of approaches are faster in decoding repetitive patterns than in compressing them. This is because they need to constantly identify repetitive patterns during the compression. However, they can decode the patterns faster since all necessary information is stored either in the tuples or in the dictionary.

In this article, we will define a reduction of an event log based on the ideas of [26] representing repetitive patterns as tuples. We will use the additional information of the tuples about the reduced pattern, i.e. reduced number of repetitions, to guide the computation of compressed alignments that can then be decoded into proper alignments for the process model.

Types of repetitive patterns. A repetitive pattern [31] is a sequence of symbols that is repeated in a given period or context, i.e. in this work the context is a given trace of an event log. The repeating sequence (a.k.a. the *repeat type*) can either be *full*, i.e. all symbols of the repeat type are repeated, or *partial*, i.e. only some symbols of the repeat type are repeated. A repeat type can either be repeated *consecutively*, i.e. all repetitions follow one another, or *gapped*, i.e. the repetitions of the repeat type occur at different positions within a given trace. In addition, a repetitive pattern can also be *approximate* with a Levenshtein distance of k symbols, i.e. the pattern allows up to k symbols disrupting the repeating sequence. In the context of conformance checking, we aim at relating a repetitive pattern to the process model to find if it can be repeated in a loop structure of the process model. For that purpose, we will rely on a restrictive class of repeat patterns, i.e. full repeat types with consecutive repetitions (a.k.a. *tandem repeats*). If the pattern were partial, approximate or gapped, the execution context of the process model would be lost and hence no cyclic behavior of the process model could be extended when decoding the repetitive patterns later on.

Repetitive patterns in process mining. In the context of process mining, repetitive patterns have been used to define trace abstractions in [8]. These trace abstractions haven then been used to discover hierarchical process models. In this context, tandem repeats have been considered for discovering loop structures and full repeat types with gapped repetitions have been used for discovering subprocesses. The properties of tandem repeats have been further explored in [8]. Specifically, a tandem repeat is called maximal, if the repeat type cannot be extended by another consecutive repetition before its starting position or after the last repetition of the tandem repeat. Conversely, a tandem repeat is called primitive, if the repeat type in itself is not another tandem repeat. These categorizations were made to discourage redundant discoveries of similar repeat types. In this article, we will hence use maximal and primitive tandem repeats to reduce the event log for the purpose of speeding up the computation of trace alignments.

3. Preliminaries

The approach presented in this paper builds on the concepts introduced in this subsection: finite state machines, Petri nets, event logs, alignments and tandem repeats.

3.1. Finite State Machines (FSM).

Our technique represents the behavior of a process model and the event log as *Finite State Machines (FSM)*. A FSM captures the execution of a process by means of edges representing activity occurrences and nodes representing execution states. Activities and their occurrences are identified by their name. Hereinafter, Σ denotes the set of labels (activity names) in both the model and the log.

Definition 3.1 (Finite state machine). *Given a set of labels Σ , a FSM is a tuple (N, A, s, R) , where N is a set of nodes, $A \subseteq N \times \Sigma \times N$ is a set of arcs, $s \in N$ is the initial node and $R \subseteq N$ is a set of final nodes. The sets N, A and R are non-empty and finite.*

An arc $a = (n_s, l, n_t) \in A$ represents the occurrence of an activity $l \in \Sigma$ at the (source) node n_s that leads to the (target) node n_t . The functions $src(a) = n_s$, $\lambda(a) = l$ and $tgt(a) = n_t$ retrieve the source node, label and target node of a , respectively. Given an arc a and a node n , we define a function $n \blacktriangleright a$ to traverse the FSM, i.e. $n \blacktriangleright a = n_t$ if $n = n_s$, and $n \blacktriangleright a = n$ otherwise. The incoming and outgoing arcs for a node n are retrieved as $\blacktriangleright n = \{a \in A \mid tgt(a) = n\}$ and $n \blacktriangleright = \{a \in A \mid src(a) = n\}$, respectively.

3.2. Petri net and reachability graph.

Process models can be represented in various modelling languages, in this work we use Petri nets due to its well-defined execution semantics. This modelling language has two types of nodes, transitions, which in our case represent activities, and places, which represent execution states. The formal definition for Petri nets is presented next.

Definition 3.2 ((Labelled) Petri net). *A (labelled) Petri net, or simply a net, is the tuple $PN = (P, T, F, \lambda)$, where P and T are disjoint sets of nodes, places and transitions, respectively; $F \subseteq (P \times T) \cup (T \times P)$ is the flow relation, and $\lambda : T \rightarrow \Sigma$ is a labelling function mapping transitions to labels $\Sigma \cup \{\tau\}$, where τ is a special label representing an unobservable action.*

Transitions with label τ represent silent steps whose execution leaves no footprint but that are necessary for capturing certain behavior in the net (e.g., optional execution of activities or loops). In a net, we will often refer to the preset or postset of a node, the preset of a node y is the set $\bullet y = \{x \in P \cup T \mid (x, y) \in F\}$ and the postset of y is the set $y \bullet = \{z \in P \cup T \mid (y, z) \in F\}$.

The work presented in this paper considers a sub-family of Petri nets: uniquely-labeled free-choice workflow nets [32, 33]. It is uniquely labelled in the sense that every label is assigned to at most one transition. Given that these nets are workflow and free choice nets, they have two special places: an initial and a final place and, whenever two transitions t_1 and t_2 share a common place $s \in \bullet t_1 \cap \bullet t_2$, then all places in the preset are common for both transitions $\bullet t_1 = \bullet t_2$. The formal definitions are given below.

Definition 3.3 (Uniquely-Labelled, free-choice, workflow net). *A (labelled) workflow net is a triplet $WN = (PN, i, o)$, where $PN = (P, T, F, \lambda)$ is a labelled Petri net, $i \in P$ is the initial and $o \in P$ is the final place, and the following properties hold:*

- i has an empty preset and o has an empty postset, i.e., $\bullet i = o \bullet = \emptyset$.
- If a transition t^* were added from o to i , such that $\bullet i = o \bullet = \{t^*\}$, then the resulting net is strongly connected.

A workflow net $WN = (P, T, F, \lambda, i, o)$ is uniquely-labelled and free-choice if the following holds:

- (Uniquely-labelled) For any $t_1, t_2 \in T$, $\lambda(t_1) = \lambda(t_2) \neq \tau \Rightarrow t_1 = t_2$.
- (Free-choice) For any $t_1, t_2 \in T$: $s \in \bullet t_1 \cap \bullet t_2 \implies \bullet t_1 = \bullet t_2 = \{s\}$.

The execution semantics of a net can be defined by means of *markings* representing its execution states and the *firing rule* describing if an action can occur. A marking is a multiset of places, i.e. a function $m : P \rightarrow \mathbb{N}_0$ that relates each place $p \in P$ to a natural number of *tokens*. A transition t is enabled at marking m , represented as $m[t]$, if each place of the preset $\bullet t$ contains a token, i.e. $\forall p \in \bullet t : m(p) \geq 1$. An enabled transition t can fire to reach a new marking m' , the firing of t removes a token from each place in the preset $\bullet t$ and adds a token to each place in the postset $t\bullet$, i.e. $m' = m \setminus \bullet t \uplus t\bullet$. A fired transition t at a marking m reaching a marking m' is represented as $m[t]m'$. A marking m' is *reachable* from m , if there exists a sequence of firing transitions $\sigma = \langle t_1, \dots, t_n \rangle$, such that $m_0[t_1] \dots m_{i-1}[t_i]m'$ holds for all $1 \leq i \leq n$.

A net with an initial and a final marking is called a (*Petri*) *system net*.

Definition 3.4 (System net). A system net SN is a triplet $SN = (WN, m_0, M_R)$, where WN is a labelled workflow net, m_0 denotes the initial marking and M_R denotes the final marking.

A marking is k -bounded if every place at a marking m has up to k tokens, i.e., $m(p) \leq k$ for any $p \in P$. A system net is k -bounded if every reachable marking in the net is k -bounded. This work considers 1-bounded system nets. Additionally, we assume that these nets are *sound* [34]: (1) from any marking m (reachable from m_0), it is possible to reach a final marking $m_f \in M_R$; (2) there is no reachable marking m from a final marking $m_f \in M_R$; and (3) each transition is enabled, at least, a reachable marking.

In this work, we further restrict the family of nets to be considered in the remaining of the paper. Specifically, we assume that the nets do not contain concurrency. Thus, any two transitions t, t' enabled at a marking m cannot be concurrent, i.e., if $m[t] \wedge m[t']$ then $\bullet t \cap \bullet t' \neq \emptyset$. This technique can be used in combination with the technique presented in [24] to deal with concurrency.

All possible markings, as well as the occurrence of observable and invisible activities, of a system net can be captured in a so-called *reachability graph* [35]. A reachability graph is a non-deterministic FSM, where nodes denote markings, and arcs denote the firing of transitions. The notation for a reachability graph will be the same as the FSM with the subscript RG , i.e., $(N_{RG}, A_{RG}, s_{RG}, R_{RG})$ is a reachability graph. In order to have a more compact representation of the reachability graph, we assume all arcs labelled with τ have been removed with the Alg. proposed in [10], thus $\lambda(a) \neq \tau$ for all $a \in A_{RG}$. The system net and reachability graph shown in Fig. 1 are going to be used as the running example throughout the paper, observe that the nodes in the reachability graph represent the markings in the net. The complexity for constructing a reachability graph of a safe Petri net is $O(2^{|P \cup T|})$ [36].

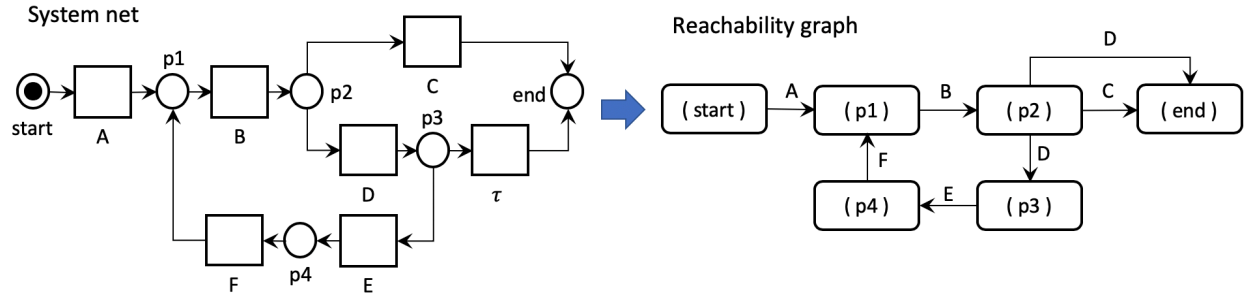


Figure 1. System net and reachability graph of the running example.

3.3. Event log and DAFSA.

Event logs record the executions of a business process. These executions are stored as sequences of activity occurrences (a.k.a. events). A sequence of events corresponding to an instance of a process is called a *trace*, where events are represented by the corresponding activity's name. Although event logs are multisets of traces, given that the same trace might have been observed several times, we are only interested in distinct traces and thus an event log is considered as a set of traces.

Definition 3.5 (Trace and Event Log). Given a set of labels Σ , a trace t is a finite sequence of labels $t = \langle l_1, l_2, \dots, l_n \rangle \in \Sigma^*$ such that $l_i \in \Sigma$ for any $1 \leq i \leq n$. An event log L is a set of traces.

The size of a trace t is defined by its number of elements and shorthand as $|t|$, while $t[i]$ retrieves the i -th element in the trace.

An event log can be represented as a FSM called *Deterministic Acyclic Finite State Automaton (DAFSA)*, as described in [10]. The DAFSA of an event log will denoted as $D = (N_D, A_D, s_D, R_D)$, with the elements listed in Def. 3.1 with subscript D . Figure 2 shows an event log, where every trace is annotated with an identifier. This identifier will be useful to keep track of the trace transformations presented in the next section.

ID	Trace
1	$\langle A, B, C, C, C, C \rangle$
2	$\langle A, B, D, E, E, F, B, D, E, E, F, B, D, E, E, F, B, C \rangle$
3	$\langle A, B, D, F, B, D, F, B, D, F, B, D \rangle$
4	$\langle A, B, D, F, B, D, F, B, D, F, B, D, F, B, D \rangle$
5	$\langle A, B, D, F, B, D \rangle$

Figure 2. Example log for our loan application process.

3.4. Alignments.

Alignments capture the common and deviant behavior between a model and a log – in our case between the FMSs representations for the model and log – by means of three operations: (1) a synchronized move (MT) traverses one arc on both FSMs with the same label, (2) a log operation (LH) and (3) a model operation (RH) that traverse an arc on the log or model FSM, respectively, while the other FSM does not move. Note that MT is commonly referred to as *match*, and LH and RH as *hides*. These operations are applied over a pair of elements that can be either arcs of the two FSMs or \perp (indicating a missing element for LH and RH). These triplets (operation and pair of affected elements) are called *synchronizations*.

Definition 3.6 (Synchronization). Let A_D and A_{RG} be the arcs of a DAFSA D and a reachability graph RG , respectively. A synchronization is a triplet $\beta = (op, a_D, a_{RG})$, where $op \in \{MT, LH, RH\}$ is an operation, $a_D \in A_D$ is an arc of the DAFSA and $a_{RG} \in A_{RG}$ is an arc of the reachability graph. The set of all possible synchronizations is represented as $S(D, RG) = \{(LH, a_D, \perp) \mid a_D \in A_D\} \cup \{(RH, \perp, a_{RG}) \mid a_{RG} \in A_{RG}\} \cup \{(MT, a_D, a_{RG}) \mid a_D \in A_D \wedge a_{RG} \in A_{RG} \wedge \lambda(a_D) = \lambda(a_{RG})\}$.

Given a synchronization $\beta = (op, a_D, a_{RG})$, the operation, the arc of the DAFSA and the arc of the reachability graph are retrieved by $op(\beta) = op$, $a_D(\beta) = a_D$ and $a_{RG}(\beta) = a_{RG}$, respectively. By the abuse of notation, let $\lambda(\beta)$ denote the label of the arc in β that is different to \perp , i.e., if $a_D(\beta) \neq \perp$ then $\lambda(\beta) = \lambda(a_D(\beta))$, otherwise $\lambda(\beta) = \lambda(a_{RG}(\beta))$.

Definition 3.7 (Alignment). An alignment is a sequence of synchronizations $\epsilon = \langle \beta_1, \beta_2, \dots, \beta_n \rangle$. The projection of an alignment ϵ to the DAFSA, shorthand as $\epsilon|_D$, retrieves all synchronizations with $a_D(\beta) = \perp$, while the projection to the reachability graph, shorthand as $\epsilon|_{RG}$, retrieves all synchronizations with $a_{RG}(\beta) = \perp$.

As a shorthand, functions op , a_D , a_{RG} and λ can be used for alignments by applying the function to each synchronization wherein. For instance, $op(\epsilon)$ results in the sequence of operations in ϵ .

An alignment is *proper* if it represents a trace t , this is $\lambda(\epsilon|_D) = t$, and both $a_D(\epsilon|_D)$ and $a_{RG}(\epsilon|_{RG})$ are paths through the DAFSA and the reachability graph from a source node to one of the final nodes, respectively. We refer to the set of all proper alignments as $\xi(D, RG)$.

Intuitively, an alignment represents the number of operations to transform a trace (path in the DAFSA) into a path in the reachability graph. An synchronizations in an alignment can be associated with a cost, the standard cost function [37, 10] is defined next, where a weight of 1 is assigned to a synchronization with *LH* and *RH* operations, and 0 to the synchronizations with *MT* operations, find the formal definition next.

Definition 3.8 (Cost function). *The cost of an alignment ϵ is $g(\epsilon) = |\{\beta \in \epsilon \mid op(\beta) \neq MT\}|$.*

3.5. Tandem repeats.

The main contribution of this paper relies on identifying and reducing the repetitive sequences of activity occurrences in the traces, *a.k.a.* tandem repeats, thus compressing each trace. A tandem repeat for a trace t is a triplet (s, α, k) , where s is the position in the trace where the tandem starts, α is the repetitive pattern, *a.k.a.* repeat type, and k is the number of repetitions of α in t . Given a trace t , $\Delta(t)$ is an oracle that retrieves the set of tandem repeats in t , such that the repeat type occurs at least twice (in other words, any tandem repeat (s, α, k) has $k \geq 2$). For the evaluation (Section 5), the approach proposed by Gusfield and Stoye [7] was used. The approach uses suffix trees to find tandem repeats in linear time with respect to the length of the input string and defines an order between the tandem repeats by reporting the leftmost occurrences first. That technique can be sped up by using suffix arrays as the underlying data structure [38]. Additionally, the tandem repeats considered in this work are *maximal* and *primitive* [8]. A tandem repeat is called maximal if no repetitions of the repeat type occur at the left or right side of the tandem repeat. The tandem repeat is primitive, if the repeat type is not itself a tandem repeat.

Definition 3.9 (Maximal and primitive tandem repeat). *A tandem repeat $(s, \alpha, k) \in \Delta$ is maximal, if there is no copy of α before s or after $s + |\alpha| * k$, and primitive if its repeat type cannot be subdivided into other repeat types.*

Figure 3 shows the primitive and maximal tandem repeats for the event log of Fig. 2. For example, in trace (1), there is one tandem repeat $(3, C, 4)$, that starts on position 3 and the sequence C is repeated 4 times. Another possible tandem repeat for trace (1) is $(3, CC, 2)$, but this is not primitive since CC is itself another tandem repeat. In the case of trace (3), $(5, BDF, 2)$ is another tandem repeat, but it is not maximal because it can be extended to the left side by one more repetition. Last, trace (3) contains another tandem repeat $(3,DFB,3)$, but it is omitted since it is the same as $(2,BDF,3)$ shifted right by one character.

ID	Maximal and primitive Tandem Repeats
(1)	$(3, C, 4)$
(2)	$(2, BDEEF, 3), (9, E, 2), (14, E, 2)$
(3)	$(2, BDF, 3)$
(4)	$(2, BDF, 4)$
(5)	$(2, BDF, 5)$

Figure 3. Primitive and maximal tandem repeats for the event log of Fig. 2.

4. Automata-based Conformance Checking with Tandem Repeats Reductions

This section presents a novel approach for computing the differences between an event log and a process model. These differences are expressed in terms of trace alignments. The proposed approach is depicted in Fig. 4. In order to increase the scalability of the approach, the first step consists in reducing the event log (Step 0.1) by finding patterns of repetition, a.k.a. *tandem repeats*, in each of the event log traces (Step 0.2). Then, the reachability graph of the process model is computed (Step 1) and, in parallel, the reduced event log is compressed into an automaton (Step 2). Finally, both automata are compared with Dijkstra’s algorithm to derive alignments representing the differences and commonalities between the log and the model (Step 3). Given that the computed alignments represent reduced event log traces, the final step (Step 4) expands those alignments to obtain the alignments of the original traces.

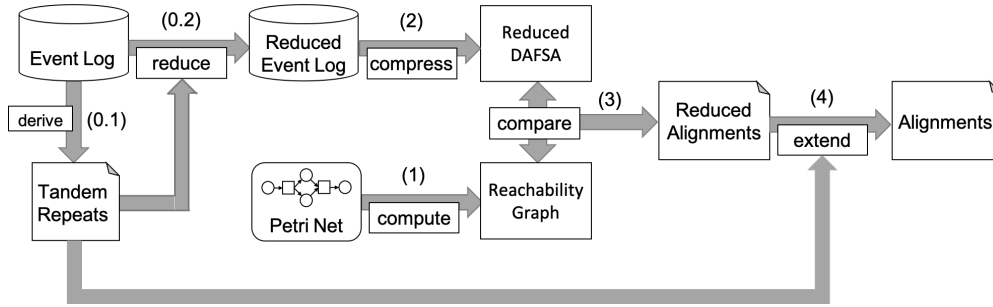


Figure 4. Overview of the Tandem Repeats Approach

4.1. Determining trace alignments with a reduced event log

The technique presented in this paper is based on the identification of primitive and maximal tandem repeats within the traces in the event log. These repeats are then reduced to two repetitions in each of the traces, producing a reduced version of the log. The alignments are then computed between the model and the reduced version of the log. The intuition behind the trace reductions is that, if the two repetitions are matched over the model, then the model is cyclic (the model is uniquely labelled) and we can assume that any additional repetition of the tandem repeat can be matched over the model.

Even though, only maximal and primitive tandem repeats are considered, they can still overlap within the trace. In order to avoid such overlapping, an order between the tandem repeats is defined, the first tandem repeats to collapse are primitive, maximal, and first to occur from left to right. The result is a reduced event log RL containing a set of reduced traces.

The reduction operation can collapse different traces into the same reduced trace. For instance, consider the traces (3) and (4) in Fig. 2, which have different number of repetitions for the same repeat type. Both tandem repeats: $(2, BDF, 3)$ and $(2, BDF, 4)$ from Fig. 3, will be reduced to only two copies, thus resulting in the reduced trace: $\langle A, B, D, F, B, D, F, B, D \rangle$, where the greyed-out areas represent the two repetitions of the token repeats. The elements in the first copy of the tandem repeats have a corresponding element in the second copy, the i -th element in the first copy is related to the i -th element in the second copy. In the example, $\langle A, B, D, F, B, D, F, B, D \rangle$, B is related to B , D with D , and F with F . In this way, when both elements, an element in the tandem repeat and its corresponding element in the second copy are matched, then a loop is found in the model.

The information about the reduction operations applied over a trace will be used later for reconstructing the original trace, thus it is important to preserve the information about the reductions applied. In order to do so, a *reduced trace* is represented as a tuple $T = (rt, p, k_{red}, TR_c, i)$, where rt is the trace to reduce, p is the order of reduction (number of reduced repetitions), k_{red} is the total number of reduced labels, TR_c relates the two repetitions of the tandem repeats: an i th element in the first repetition is related to the i th element in the second repetition, and i is an auxiliary index representing the position in the trace from which tandem repeats can be identified. Finally, *Reductions* relates each trace to its reduced version. Observe that a trace t with no tandem repeats, or prior a reduction, is $(t, \emptyset, 0, \emptyset, 1)$ where t is a trace and the tandem repeats shall be identified from position 1. The next definition formalises the *trace reduction* operation.

Definition 4.1 (Maximal trace reduction). Let $T = (t, p, k_{red}, TR_l, i)$ be a – possibly reduced – trace and $(s, \alpha, k) \in TR(t, i)$ be a maximal tandem repeat, such that $\nexists (s_i, \alpha_i, k_i) \in TR(t, i) : |\alpha_i| * k_i > |\alpha| * k$. The reduced T by k is $\gamma(T) = (rt, p', k'_{red}, TR'_l, i')$, where:

- $rt \leftarrow Prefix(t, i - 1) \oplus \alpha \oplus \alpha \oplus Suffix(t, i + (|\alpha| * k))$,
- $p' \leftarrow p \cup \{j \rightarrow k - 2 \mid i \leq j \leq (i + |\alpha| * 2 - 1)\}$,
- $k'_{red} \leftarrow k_{red} + (k - 2) * |\alpha|$,
- $TR'_c \leftarrow TR_c \cup \{j \rightarrow j + |\alpha|, j + |\alpha| \rightarrow j \mid i \leq j \leq (i + |\alpha| - 1)\}$, and
- $i' \leftarrow i + |\alpha| * 2$.

The reduction of a given event log and its tandem repeats is displayed in Alg. 1. Each trace $t \in L$ is reduced from position i until no more tandem repeats can be found and reduced and i reaches the end of the trace $|t|$. Algorithm 1 returns the reduced log RL and the reduction information $Reductions$.

Algorithm 1: Reduce event log

input: Event log L ; Tandem repeats $TR(t)$ for each $t \in L$

```

1 Set  $RL \leftarrow Reductions \leftarrow \{\}$ ;
2 for  $t \in L$  do
3   Set  $i = 1$ ;
4   Set  $rTrace = (t, \emptyset, 0, \emptyset, 1)$ ;
5   while  $i \leq |t|$  do
6     Set  $rTrace = \gamma(rTrace)$ ;
7     if  $i = rTrace[5]$  then Increase  $i$  by 1;
8     else Set  $i \leftarrow rTrace[5]$ ;
9     Set  $rTrace[5] \leftarrow i$ ;
10   $RL \leftarrow RL \cup \{t\}$ ;
11   $Reductions \leftarrow Reductions \cup \{t \rightarrow rTrace\}$ ;
12 return  $RL, Reductions$ ;
```

Figure 5 shows the reduced event log for our running example after applying Alg. 1. For example, trace (4) was reduced to the trace $\langle A, B, D, F, B, D, F, B, D \rangle$ by reducing the tandem repeat at position 2 with length 3, the labels reduced are $k_{red} = 6$, function TR_c relates positions 2 and 5, 3 and 6, and so on and so forth.

ID	Reduced Trace	P	k_{red}	TR_c	pos
(1)	$\langle A, B, C, C \rangle$	$3 - 4 \rightarrow 2$	2	$3 \leftrightarrow 4$	4
(2)	$\langle A, B, D, E, E, F, B, D, E, E, F, B, C \rangle$	$2 - 11 \rightarrow 1$	5	$2 - 5 \leftrightarrow 6 - 11$	12
(3)	$\langle A, B, D, F, B, D, F, B, D \rangle$	$2 - 7 \rightarrow 1$	3	$2 - 4 \leftrightarrow 5 - 7$	9
(4)	$\langle A, B, D, F, B, D, F, B, D \rangle$	$2 - 7 \rightarrow 2$	6	$2 - 4 \leftrightarrow 5 - 7$	9
(5)	$\langle A, B, D, F, B, D, F, B, D \rangle$	$2 - 7 \rightarrow 3$	9	$2 - 4 \leftrightarrow 5 - 7$	9

Figure 5. Reduced event log after applying Alg. 1.

Next, we compute the alignments between the reachability graph and the DAFSA of the reduced event log. In order to compute these alignments, the algorithm in [10] is adapted in two ways for dealing with reduced traces. First, the cost function in Def. 3.8 is modified, this will be critical when the computed alignments are extended to full alignments for the original traces. Second, for improving the computation time, a binary search is implemented for traces reduced to the same reduced trace.

4.1.1. Cost function

The cost function is modified to consider the amount of reduced tandem repeats. Specifically, even though several traces can have the same reduced trace, their alignment with a path in the reachability graph can have different costs. Consider the case when an element in a tandem repeat needs to be hidden (*LH*), and this hiding operation is required in every repetition of the element. Thus, the more it is repeated in a trace (the higher the reduction factor in the reduced trace), the higher the cost for the computed alignment. The cost of an alignment involving a reduced trace needs to consider different cases: if a synchronization does not involve an element in a tandem repeat, then the cost is the usual (0 for *MT* and 1 otherwise); whereas if it involves an element in a tandem repeat, then it is necessary to determine if the element is loopable in the reachability graph and can be synchronized in all repetitions.

Definition 4.2 shows the modified cost function. By the abuse of notation, we use *s..end* to create a sequence of numbers from *s* to *end* with an increment of 1. Given a sequence *t*, we use *Prefix(t, i)* to refer to the prefix of sequence *t* from position 1 to *i*, and *Suffix(t, i)* to refer to the suffix of sequence *t* from position *i* to *|t|*. Let *pos_t* be a function relating each index *i* of an alignment, where $1 \leq i \leq |\epsilon|$, to the trace position that has been aligned up to, then $pos_t(\epsilon, i) = |\{\beta \in Prefix(\epsilon, i) \mid op \neq RH\}|$. For the other direction, we define a function *pos_ε* that given a trace position *j* returns the exact position in an alignment ϵ where the trace label is aligned, i.e. $pos_\epsilon(\epsilon, j) = \min\{1 \leq i \leq |\epsilon| : pos_t(\epsilon, i) = j\}$. For assigning the additional cost, we use function *p* (Def. 4.1) relating each trace index of a tandem repeat to the number of reduced repetitions. We complete the definition of this function by relating all remaining trace indices to 0, i.e. $p \leftarrow p \cup \{j \rightarrow 0 \mid 1 \leq j \leq |rt| \wedge j \notin dom(p)\}$ for every $rt \in RL$.

So far the cost function for reduced alignments assigns a value of $1 + p(pos_t(\epsilon, i))$ to all synchronizations that are hide operations and 0, otherwise. For each complementary pair of positions of a tandem repeat, an additional cost is assigned at most once, even if both labels are aligned with a *LH* operation. This ensures that hiding all labels of a tandem repeat with *LH* operations results in the same cost as if all labels in the extended tandem repeat were hidden with the traditional cost function from Def. 3.8. For implementing this idea, we rely on the complement function *TR_c* from Def. 4.1 that links each trace position to its complementary position of its tandem repeat. We extend this function to also apply to alignments (denoted as *TR_c(ε, i)*), which given a position *i* in alignment ϵ , first retrieves its trace position with function *pos_t*, second retrieves the complementary trace position with function *TR_c* and finally retrieves the position of the complement in the alignment with function *pos_ε*, i.e. $TR_c(\epsilon, i) = pos_\epsilon(TR_c(pos_t(\epsilon, i)))$. We cover the case of two *LH* operations for two complementary trace labels by only altering the cost of the element in the second copy, i.e. where the trace position is larger than the complement position ($TR_c(\epsilon, i) < pos_t(\epsilon, i)$). If both the operation at position *i* and at the complementary position in the alignment $TR_c(\epsilon, i)$ are *LH*, then the cost of the alignment position *i* is reduced to one. Now, we can introduce the cost function of a reduced alignment as follows:

Definition 4.2 (Cost function of a reduced alignment). *Given an alignment ϵ , the function *p* for relating trace indices to the number of reduced repetitions, the function *TR_c* that links each trace position of a tandem repeat to its complement and a position *i* within ϵ , we define the cost of a synchronization in alignment ϵ with function *f* as follows:*

$$f(\epsilon, p, TR_c, i) = \begin{cases} 1, & \text{if } p(pos_t(\epsilon, i)) \geq 1 \wedge TR_c(\epsilon, i) < pos_t(\epsilon, i) \\ & \text{and } op(\epsilon[i]) = LH \wedge op(\epsilon[TR_c(\epsilon, i)]) = LH \\ 1 + p(pos_t(\epsilon, i)), & \text{if } op(\epsilon[i]) = RH \vee op(\epsilon[i]) = LH \\ 0, & \text{if } op(\epsilon[i]) = MT \end{cases}$$

The total cost ρ for a reduced alignment is the sum of *f* for each element in the alignment ϵ

$$\rho(\epsilon, p, TR_c) = \sum_{i \in 1..|\epsilon|} f(\epsilon, p, TR_c, i)$$

Figure 6 shows an alignment for the reduced trace (3) in Fig. 5 and the computation for the cost function with all its auxiliary functions. The alignment can match all the trace labels of the reduced trace, but has to hide label E with a RH operation when traversing the loop B, D, E, F in the process model. The trace position does not move during the RH synchronization at alignment position 4, i.e. function $pos_t(\epsilon, i)$ is still at position 3. Since the alignment does not contain any LH synchronizations, the complement functions do not influence the cost of this alignment. One point of interest, however, is that the trace complement $TR_c(pos_t(\epsilon, i))$ of position 2 points to trace position 5 while the alignment complement $TR_c(\epsilon, i)$ points to the alignment position 6 (because $RH(E)$ was aligned in between). Since one repetition has been reduced ($p(pos_t(\epsilon, i))$), the cost for each of the two RH synchronizations is 2 because they are contained in a tandem repeat ($f(\epsilon, p, TR_c, i)$). The cost of the reduced alignment is 4. Please note that this cost over estimates the optimal cost of the extended alignment, which is 3 for the sequence $\langle MT(B), MT(D), RH(E), MT(F) \rangle$ inserted after position 5 and before 6. However, this does not pose a problem since this fact only discourages on overly use of RH synchronizations to construct large repetitive sequences while the extension algorithm (presented later) properly constructs the extended alignment with the correct cost.

pos i	1	2	3	4	5	6	7	8	9	10	11
ϵ	$MT(A)$	$MT(B)$	$MT(D)$	$RH(E)$	$MT(F)$	$MT(B)$	$MT(D)$	$RH(E)$	$MT(F)$	$MT(B)$	$MT(D)$
rt	A	B	D		F	B	D		F	B	D
$pos_t(\epsilon, i)$	1	2	3	3	4	5	6	6	7	8	9
$TR_c(pos_t(\epsilon, i))$		5	6		7	2	3		4		
$TR_c(\epsilon, i)$		6	7		9	2	3		5		
$p(pos_t(\epsilon, i))$	0	1	1	1	1	1	1	1	1	0	0
$f(\epsilon, p, TR_c, i)$	0	0	0	2	0	0	0	2	0	0	0
$\rho(\epsilon, p, TR_c)$	4										

Figure 6. Cost of the reduced alignment of trace (3) from the running example.

Different from other approaches, this work uses Dijkstra algorithm to find optimal alignments instead of an A^* -search as other approaches. The adaptation of this work to an A^* -search is left for future work.

4.1.2. Binary search

Given that several original traces are reduced to the same reduced trace, a binary-style search is implemented for computing the alignments. This search starts by taking all original traces that share the same reduced trace, and ordering them in an ascending order with respect to the total number of reduced labels (k_{red} from Def. 4.1), which will define an interval with the reduced traces with lowest and highest number of reduced labels on the extremes. The binary search proceeds by computing the alignments for the reduced traces, it starts by taking the two reduced traces with the lowest and highest number of reduced labels. The search stops when the alignments for both – lowest and highest reduced labels – are equal (i.e. involve the same synchronizations) and, if there is any reduced traced between them wr.t. the order, then it will get the same alignment. In case the alignments are not equal, the search continues by splitting the interval into two, investigating one interval from the lowest value of k_{red} to the average and one interval from the average to the highest value of k_{red} until all alignments have been computed (either implicitly as part of an interval or as explicitly as a border of an interval).

For example, traces (3) to (5) in Fig. 5 are an interval for the binary search as their reduced traces are the same. The traces are already sorted according to k_{red} , next the alignments are computed for traces (3) and (5) with the lowest and highest numbers of k_{red} , respectively. Both reduced traces lead to the same alignment as reported in Fig. 6 and the computation of the alignment for trace (4) can be omitted.

The binary search is described in Alg. 2, it starts by sorting all original trace reductions for a given reduced trace according to their overall number of reduced labels k_{red} . Please note that we use $\uparrow x$ to

formalize sorting a set into a sequence by using the order of variable x in ascending order. We start with the largest interval from the minimum to the maximum number of repetitions. Then we calculate a reduced alignment for the lower and one for the upper border and store them in a function \mathcal{A} relating trace reductions to alignments of reduced traces (to prevent re-computing alignments when the interval needs to be split). If the alignment of the lower equals the alignment of the upper border, then all intermediate trace reductions relate to the same reduced alignment. Otherwise, the binary search continues with the two new intervals, one from the lower to the average and another from the average to the upper number of reduced labels. This binary search continues until all open intervals have been investigated, which in the worst-case computes one reduced alignment for each trace reduction. For the function align, we refer to [24]. In this article, we use the adjusted cost function according to Def. 4.2.

Algorithm 2: Binary search for computing reduced alignments

input: Reduced event log RL ; Reductions $Reductions$; Reduced DAFSA $FSM_{D,red}$; Reachability Graph RG

```

1  $\mathcal{A} \leftarrow \{\}$ ;
2 for  $t \in RL$  do
3    $rTrace \leftarrow \langle (rt, p, k_{red}, TR_c) \in val(Reductions) \mid rt = t \wedge \uparrow k_{red} \rangle$ ;
4    $Pairs \leftarrow \{(1, |rTrace|)\}$ ;
5   while  $Pairs \neq \emptyset$  do
6      $(lo, up) \leftarrow$  remove an element from  $Pairs$ ;
7     if  $\mathcal{A}(rTrace(lo)) = \perp$  then
8        $\mathcal{A} \leftarrow \mathcal{A} \cup \{rTrace(lo) \rightarrow align(rTrace(lo), FSM_{D,red}, RG)\}$ ;
9     if  $\mathcal{A}(rTrace(up)) = \perp$  then
10       $\mathcal{A} \leftarrow \mathcal{A} \cup \{rTrace(up) \rightarrow align(rTrace(up), FSM_{D,red}, RG)\}$ ;
11     if  $\mathcal{A}(rTrace(lo)) = \mathcal{A}(rTrace(up))$  then
12       for  $i \in lo..up$  do  $\mathcal{A} \leftarrow \mathcal{A} \cup \{rTrace(i) \rightarrow \mathcal{A}(rTrace(lo))\}$ ;
13     else  $Pairs \leftarrow Pairs \cup \{(lo, \lfloor (lo + up)/2 \rfloor), (\lceil (lo + up)/2 \rceil, up)\}$ ;
14 return  $\mathcal{A}$ ;
15 Function  $align((t, p, k_{red}, TR_c), D, RG)$ 
16    $o \leftarrow \{((s_D, s_{RG}, \langle \rangle), \rho(\langle \rangle, p, TR_c))\}$ ;
17   while  $o \neq \emptyset$  do
18      $n_{act} \leftarrow$  remove  $(n_D, n_{RG}, \epsilon)$  from  $o \mid \nexists (n', \rho')$  with  $\rho' < \rho(\epsilon, p, TR_c)$ ;
19     if  $c(n_D, n_{RG}) = \perp \vee c(n_D, n_{RG}) \geq \rho(\epsilon, p, TR_c)$  then
20        $c \leftarrow c \cup \{(n_D, n_{RG}) \rightarrow \rho(\epsilon, p, TR_c)\}$ ;
21     else Continue;
22     if  $n_D \in R_D \wedge n_{RG} \in R_{RG} \wedge \lambda(\epsilon|_D) = t$  then return  $\epsilon$ ;
23     else
24       for  $a_D \in n_D \blacktriangleright \lambda(a_D) = t(|\epsilon|_D(\epsilon)| + 1)$  do
25          $o \leftarrow o \cup \{(tgt(a_D), n_{RG}, \epsilon \oplus (LH, a_D, \perp))\}$ ;
26         for  $a_{RG} \in n_{RG} \blacktriangleright \lambda(a_{RG}) = \lambda(a_D)$  do
27            $o \leftarrow o \cup \{(tgt(a_D), tgt(a_{RG}), \epsilon \oplus (MT, a_D, a_{RG}))\}$ ;
28       for  $a_{RG} \in n_{RG} \blacktriangleright$  do  $o \leftarrow o \cup \{(n_D, tgt(a_{RG}), \epsilon \oplus (RH, \perp, a_{RG}))\}$ ;

```

4.2. Extending Reduced Trace Alignments

This subsection describes how reduced alignments are extended to full and proper alignments, which represent the original traces. Every tandem repeat compressed during the trace reduction step is inserted back into the reduced alignment. They are inserted between the synchronizations of the two copies of the tandem repeats preserved in the reduced trace. In order to be considered a valid alignment, the insertion of the compressed tandem repeats shall form a valid path through the reachability graph when inserted into the reduced alignment.

The alignment of a reduced trace extends each of the token repeats in order, as observed in the trace, from right to left. Having identified the start of the first and second copy of a tandem repeat to expand, $TR_{s,1}(\epsilon, i)$ and $TR_{s,2}(\epsilon, i)$, respectively, Then, the middle copy needs to be inserted between the first and second aligned copies of the tandem. If several repetitions of the tandem repeat have been reduced, the middle copy has to be inserted repeatedly in between the two copies until the original trace is reconstructed. For finding the middle copy, the leftmost alignment position j in the first tandem repeat copy is identified, where both j and its complement in the second copy $TR_c(\epsilon, j)$ have been aligned with a *MT* operation. Since the underlying system net is uniquely labelled, we know that all synchronizations in between these two aligned positions necessarily form a loop, and this sequence can be repeatedly executed on the process model. We also know that the sequence involves all trace labels of the tandem repeat since the complement function denotes the first and second occurrence of one specific label of the repeat type and all other labels of the repeat type need to occur in between. However, the trace labels of the identified repeatable sequence might not be in the order of the tandem repeat. The middle copy is then constructed by rotating the repeatable sequence until the first label of the tandem repeat is at the first position. This is achieved by first taking the sequence from the start of the second copy ($TR_{s,2}(\epsilon, i)$) up to the end of the repeatable sequence in the second copy ($TR_c(\epsilon, j)$) and then adding the sequence after j from the first copy up to the end of the first copy ($TR_{s,2}(\epsilon, i) - 1$). If no repeatable sequence can be identified, we construct the middle copy consisting of all *LH* and *MT* synchronizations from the first copy and change their operation to *LH* to represent all trace labels of the tandem repeat but to not change the path through the process model. After inserting the middle copies, we update functions TR_c and p by removing the reference to the extended tandem repeat and move position i left to one position before the start of the first copy. We can now present the formal definition of an extended alignment:

Definition 4.3 (Extended alignment). *Let $E = (\epsilon, TR_c, p, i)$ be a - possibly extended - alignment and the trace position of i is the last position of a tandem repeat to be extended, i.e. $pos_t(\epsilon, i) \in dom(TR_c)$. The two copies of this tandem repeat ϵ_1 and ϵ_2 can be identified as two sequences in ϵ as follows:*

- $\epsilon_1 = \epsilon[TR_{s,1}(\epsilon, i)..TR_{s,2}(\epsilon, i) - 1]$
- $\epsilon_2 = \epsilon[TR_{s,2}(\epsilon, i)..i]$

A sequence within ϵ_1 and ϵ_2 can be characterized as repeatable by a single position k if both alignment positions k and its complement $TR_c(\epsilon, k)$ are *MT* operations. The left most position of a repeating sequence j is defined as:

- $j = \min\{k \in TR_{s,1}(\epsilon, i)..TR_c(\epsilon, i) \mid op(\epsilon[k]) = MT \wedge op(\epsilon[TR_c(\epsilon, k)]) = MT\}$

Depending, if there exists a repeating sequence in the two copies (i.e. $j > 0$), a middle copy for the extension can be defined as follows:

- $\epsilon_{mid} = \begin{cases} \epsilon[TR_{s,2}(\epsilon, i)..TR_c(\epsilon, j)] \oplus \epsilon[j+1..TR_{s,2}(\epsilon, i) - 1], & \text{if } j > 0 \\ \langle (LH, a_D(\beta), \perp) \mid \beta \in \epsilon_1 \wedge op(\beta) \neq RH \rangle, & \text{Otherwise} \end{cases}$

Then the extended alignment is $\Gamma(E) = (\epsilon_{ext}, TR'_c, p', i')$, where:

- $\epsilon_{ext} \leftarrow Prefix(\epsilon, TR_{s,1}(\epsilon, i) - 1) \oplus \epsilon_1 \oplus \langle \epsilon_{mid} \rangle^{p(pos_t(\epsilon, i))} \oplus \epsilon_2 \oplus suff(\epsilon, i)$
- $TR'_c \leftarrow TR_c \setminus \{k \rightarrow TR_c(k), TR_c(k) \rightarrow k \mid k \in pos_t(\epsilon, TR_{s,1}(\epsilon, i))..TR_c(pos_t(\epsilon, i))\}$
- $p' \leftarrow p \oplus \{k \rightarrow 0 \mid k \in pos_t(\epsilon, TR_{s,1}(\epsilon, i))..pos_t(\epsilon, i)\}$
- $i' \leftarrow TR_{s,1}(\epsilon, i) - 1$

Algorithm 3 describes the procedure to fully extend the reduced alignments. The aim is to create a mapping \mathcal{A}_{ext} that maps each original trace of the event log to its full alignment. Each reduced alignment is extended by moving from right to left with a counter i , and extending each encountered tandem repeat by applying the extension in Def. 4.3. If no tandem repeat is to be extended then we decrease the position by 1. This procedure gets repeated until all tandem repeats have been extended and the counter i reaches the start of the alignment.

Algorithm 3: Extending reduced alignments

input: Event log L ; Reductions $Reductions$; Reduced alignments \mathcal{A} ;

```

1  $\mathcal{A}_{ext} \leftarrow \{\}$ ;
2 for  $t \in L$  do
3    $rTrace = (rt, p, k_{red}, TR_c) \leftarrow Reductions(t)$ ;
4    $\epsilon \leftarrow \mathcal{A}(rTrace)$ ;
5    $i \leftarrow |\epsilon|$ ;
6    $E \leftarrow (\epsilon, TR_c, p, i)$ ;
7   while  $i \geq 1$  do
8     Set  $E \leftarrow \Gamma(E)$ ;
9     if  $i = E[4]$  then Decrease  $i$  by 1;
10    else Set  $i \leftarrow E[4]$ ;
11    Set  $E[4] \leftarrow i$ ;
12   $\mathcal{A}_{ext} \leftarrow \mathcal{A}_{ext} \cup \{t \rightarrow E[1]\}$ ;
13 return  $\mathcal{A}_{ext}$ ;
```

Figure 7 shows the extension of the reduced alignment ϵ for the reduced trace (3) in Fig. 5. Algorithm 3 moves backwards from alignment position 11 to position 9, which is the last position of the reduced tandem repeat B, D, F . Next, the positions of the two copies of the tandem repeat (both highlighted with grey background colour in the figure) are identified in the alignment. The first copy starts at position $TR_{s,1}(\epsilon, \hat{i}) = 2$ and continues up to position $TR_c(\epsilon, i) = 5$, while the second copy starts at position $TR_{s,2}(\epsilon, i) = 6$ and ends at position $i = 9$. A repeatable sequence can be identified at position $j = 2$ since both position 2 and its complementary position $TR_c(\epsilon, j) = 6$ are aligned with MT operations. The middle copy then can be constructed from the prefix of the second copy up to and including position 6, which is $MT(B)$, and then adding the suffix from the first copy after position 2, i.e. $MT(D), RH(E), MT(F)$. This middle copy is then inserted after the end of the first copy at position 5 to extend the reduced alignment.

pos i	1	2	3	4	5					6	7	8	9	10	11
ϵ	$MT(A)$	$MT(B)$	$MT(D)$	$RH(E)$	$MT(F)$					$MT(B)$	$MT(D)$	$RH(E)$	$MT(F)$	$MT(B)$	$MT(D)$
Functions		$TR_{s,1}(\epsilon, \hat{i})$			$TR_c(\epsilon, i)$					$TR_{s,2}(\epsilon, i)$			i		
Repeatable		j								$TR_c(\epsilon, j)$					
ϵ_{mid}						$MT(B)$	$MT(D)$	$RH(E)$	$MT(F)$						
ϵ_{ext}	$MT(A)$	$MT(B)$	$MT(D)$	$RH(E)$	$MT(F)$	$MT(B)$	$MT(D)$	$RH(E)$	$MT(F)$	$MT(B)$	$MT(D)$	$RH(E)$	$MT(F)$	$MT(B)$	$MT(D)$

Figure 7. Extending the reduced alignment of trace (3) from the running example.

The following lemma shows that the extended alignments are proper alignments: they describes traces in the log and paths through the reachability graph.

Lemma 4.1 (An extended alignment is a proper alignment). *Given a trace $t \in L$, the alignment ϵ_{ext} , returned by Alg. 3, is a proper alignment. Thus, the following two properties hold for ϵ_{ext} :*

1. *the labels in the synchronizations related to the DAFSA represent the trace, i.e. $\lambda(\epsilon|_D(\epsilon_{ext})) = t$, and*
2. *the arcs in the synchronizations related to the reachability graph forms a path through the reachability graph, i.e., for $path = a_{RG}(\epsilon|_{RG}(\epsilon_{ext}))$ holds $src(path(1)) = s_{RG} \wedge tgt(path(|path|)) \in R_{RG} \wedge \forall i \in 1..|path| - 1 : tgt(path(i)) = src(path(i + 1))$.*

The sketch of proof can be found in the Appendix A.1. As a result of the Lemma 4.1, every extended alignment will never underestimate the minimal cost of an alignment.

Proposition 4.1. *The cost of an extended alignment is minimal or higher*

4.3. Handling Concurrency in Process Models

The presented technique can be used in combination with [24] to deal with models with parallelism. [24] proposes a decomposition-based approach for conformance checking. It decomposes a process model with concurrency into its S-Components, which are concurrency-free sub-models. In such conformance checking approach, the event log is split into sub-logs, one per S-Component. Each of such sub-logs is created by filtering out the activities not present in a corresponding S-Component. Each pair of S-Component and sub-log is transformed into its an automaton, and alignments are computed for each pair. Finally, decomposed alignments are recomposed into proper alignments for the original traces with an approximate cost. For detailed explanations of each step, we refer to [24].

Figure 8 shows the integration between the tandem repeat reductions and S-Component based approach for the computation of alignments. First, the model is decomposed into S-Components and the the sub-logs are created for each S-Component (as specified in [24]), then given that the S-Components are concurrency-free, we detect and reduce tandem repeats for each sub-log. Thus, Alg. 2 is applied to each pair of S-Component and reduced sub-log to derive reduced and decomposed alignments. These alignments are then extended with Alg. 3 and then recomposed with the procedure described in [24]. The resulting alignments are proper and of approximate cost.

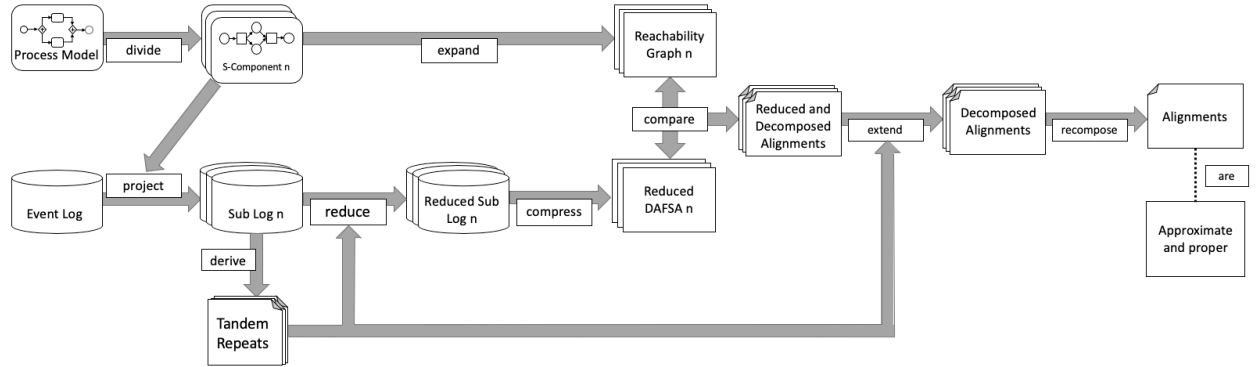


Figure 8. Integrating tandem repeats with the S-Components approach

5. Evaluation

We implemented our technique as a standalone open-source command-line tool¹ as part of the Apromore process mining environment [39]. Given an event log in XES format and a process model in either BPMN or PNML format, the tool produces various alignment statistics such as fitness and raw fitness costs. Optionally, the tool can output the alignments found or manifest the PSP data structure. It is also possible to specify which extension to the Automata-based approach should be applied, i.e. i) base approach without any extension (Automata); ii) with the S-Components extension (SComp); iii) with the S-Components and tandem repeats reduction (TR-SComp); or iv) a hybrid approach that tries to automatically select the most suitable extension based on the characteristics of the input model and log (Hybrid).

Using this tool, we evaluated the time performance and accuracy of our technique in a series of experiments, against two internal baselines (Automata and SComp), and three external baselines. For the external baselines, we chose two exact and one approximate approach for computing trace alignments: (1) the newest version of the trace alignment technique presented in [37] using the ILP marking equation and implemented in the PNetReplayer package of ProM² (ILP); (2) the extended version of the trace alignment approach presented in [4] using the extended marking equation, which is also implemented in the PNetReplayer package of ProM (eMEQ); and (3) an approximate approach using local search to compute alignments of large instances presented in [15] (ALI). While the approximate approach ALI is only implemented as a Python prototype,³ the authors previously compared it with the two exact baselines for optimal alignments computation, and showed to outperform these on a synthetic dataset [15]. We conducted the experiments for ALI with the commercial ILP solver Gurobi.

5.1. Setup

For the purpose of measuring time performance, we recorded the execution time of our technique and of the four baselines by computing the alignments of a range of model-log pairs. Each experiment was repeated five times and we reported the average execution time of runs #2–#4 to exclude the influence of the Java class loader and to reduce variance. For practical reasons, we set a time bound of ten minutes for each measurement taking into account the worst-case exponential time complexity of computing alignments. We note that previous experiments reported that in certain cases the computation of an alignment may take over a dozen hours [20]. However, setting such large time bound would have rendered this evaluation impractical, given the very large number of model-log pairs.

As for accuracy, we measured the alignment cost per trace (cf. Def. 3.8) for each model-log pair. This allows us to assess the degree of optimality of the different approximate techniques. We chose alignment cost over other conformance measures such as fitness as cost allows us to better pinpoint over-approximation. We conducted these experiments on a single-threaded 22-core Intel Xeon CPU E5-2699 v4 with 2.30GHz and with 128GB of RAM running JVM 8.

5.2. Datasets

In terms of datasets, we used a range of public and private log-model pairs from a recent benchmark on automated process discovery [40]. The publicly available dataset consists of twelve event logs, which originate from the 4TU Centre for Research Data.⁴ It consists of logs from the Business Process Intelligence challenge (BPIC) series, i.e. BPIC12 [41], BPIC13_{cp} [42], BPIC13_{inc} [43], BPIC14 [44], BPIC15 [45], BPIC17 [46], the Road Traffic Fines Management process log (RTFMP) [47] and the SEPSIS Cases log (SEPSIS) [48]. The BPIC logs from years 2011 and 2016 (BPIC11 and BPIC16) were excluded since they do not represent real business processes. We extended this dataset with the BPIC logs from the years 2018 (BPIC18) and 2019 (BPIC19), which were published after the benchmark paper. As suggested by the description of BPIC19, we

¹The tool, the public logs and models used as input, and the experiment results are available at <https://apromore.org/platform/tools>

²Available at <http://www.promtools.org>

³Available at <https://www.cs.upc.edu/~taymouri/tool.html>

⁴https://data.4tu.nl/repository/collection:event_logs_real

split this log into four sublogs according to the attribute item category since the log captures four different types of processes. Hence, the public dataset was extended to a total of 17 event logs. These public logs cover process executions from different domains such as finance, healthcare, government and IT service management.

The private dataset from [40] encompasses eight proprietary logs. These originate from several organizations around the world, including healthcare, banking, insurance and software vendors.

The authors of the benchmark in [40] could not discover process models for two of the public event logs (BPIC15 and BPIC17) since the majority of automated discovery techniques used in this benchmark exceeded the allotted memory (i.e. they ran into a state-space explosion). To overcome this problem, they applied the filtering technique described in [49] to filter infrequent behavior. We retained this filtering step to ensure compatibility with the dataset used in the benchmark paper (in the results, these filtered logs are annotated with “ f ”). As for the logs BPIC18 and BPIC19, we were also unable to discover process models using the unfiltered logs. In contrast to the benchmark paper, also the filtering technique could not be applied in a reasonable time frame. Thus, we decided to apply a naive filter to remove all traces that occur only once in order to obtain a process model for these two logs. When comparing the logs with the discovered process models for alignment computation, however, we retained the unfiltered logs, so as to detect more complex alignments.

In Table 1 we report the log characteristics as well as a range of statistics related to the application of the tandem repeats reduction. The size of the logs differs in terms of total number of events (5.9K to 2.5M) and traces (681 to 788K). Particularly relevant for the computation of alignments are the number of unique (“Unq.”) events (4–74), the number of unique traces (128–28K) and the average (“Ø”) and maximum (“Max”) trace length (“|Trace|”, average 3.4–64, maximum 9–2,973). These statistics are closely linked with the complexity of computing alignments since they determine the number and length of alignments to be computed. These logs thus feature a wide range of characteristics, including both simple and complex logs.

To quantify the degree of repeated behavior, we also report various measures related to tandem repeats in Table 1. Specifically, we report the average (“Ø”) number of identified tandem repeat tuples per trace (“#TRs”, 0–2.47); the average number of repetitions per tandem repeat (“Reps”, 0–8.11); and the average length of the repeating sequence (length, 0–1.72). Next, we show the results of reducing the event logs also using our reduction algorithm (cf. Alg. 1). Specifically, we report the average and maximum trace length before (“|Trace|”) and after reduction (“|Trace TR|”). We can observe that on average each trace is reduced by 2.3 events across all logs.⁵ In particular, for the BPIC12 log, we had the highest average reduction per trace (14 events) with the longest trace being reduced from 175 to 117 events (“Max”). One extreme case can be observed in BPIC18, where the longest trace of 2,973 events was reduced to 1,535 events (about half its length). Another effect of the tandem repeat reduction is that some reduced traces can be mapped to the same unique trace resulting in a smaller number of unique traces (“Unq. TR”), and so less alignments to compute. On average across all event logs around 500 unique traces were reduced. Two interesting examples are BPIC12 and BPIC17_f, where the number of unique traces could be reduced by 2,086 and respectively 6,119 traces, highlighting the benefits of the binary search (cf. Alg. 2).

The automated process discovery benchmark [40] used four state-of-the-art automated discovery methods, namely: Inductive Miner (IM)[50], Split Miner (SM) [51], Structured Heuristics Miner [52] and Fodina [53]. We discarded the process models discovered by the latter two methods since they may lead to process models with transitions with duplicate events (and in some cases also to unsound models), which are not supported by our technique. This resulted in a total of 40 log-model pairs from the benchmark dataset. We then discovered two process models for BPIC18 and eight process models for the four sublogs of BPIC19, using the latest version of Split Miner and Inductive Miner, giving rise to ten additional models. This resulted in a total of 50 model-log pairs for our evaluation.

In Table 2 we provide the characteristics of the process models discovered by Inductive (IM) and Split Miner (SM). For these models, we report the overall size as the sum of places, transitions and arcs (“Size”), as well as the number of transitions (“Trns.”), choices (“XOR”) and parallel splits (“AND”), and the size of

⁵We observe that this statistic includes both traces with and traces without repeated events.

Log	#Events		#Traces		Trace		Tandem repeats (\emptyset)			#Traces		Trace TR	
	Overall	Unq.	Overall	Unq.	\emptyset	Max	#TRs	Reps	length	Unq.	TR	\emptyset	Max
BPIC12	262,200	24	13,087	4,366	41.8	175	2.27	8.11	1.05	2,280	27.8	117	
BPIC13 _{cp}	6,660	4	1,487	183	9.9	35	0.63	4.3	1.25	120	8.2	25	
BPIC13 _{inc}	65,533	4	7,554	1,511	19.2	123	1.19	4.71	1.27	992	15.4	104	
BPIC14 _f	369,485	9	41,353	14,948	15.5	167	0.22	3.8	1.19	14,477	15.1	165	
BPIC15 _{1f}	21,656	70	902	295	35.1	50	0.0	0.0	0.0	295	35.1	50	
BPIC15 _{2f}	24,678	82	681	420	42.4	63	0.0	0.0	0.0	420	42.4	63	
BPIC15 _{3f}	43,786	62	1,369	826	34.6	54	0.0	0.0	0.0	826	34.6	54	
BPIC15 _{4f}	29,403	65	860	451	36.6	54	0.0	0.0	0.0	451	36.6	54	
BPIC15 _{5f}	30,030	74	975	446	42.1	61	0.0	0.0	0.0	446	42.1	61	
BPIC17 _f	714,198	18	21,861	8,767	38.1	113	2.47	5.41	1.04	2,648	29.5	73	
RTFMP	561,470	11	150,370	231	8.2	20	0.15	6.32	1.0	202	7.5	11	
SEPSIS	15,214	16	1,050	846	16.3	185	0.15	3.58	1.54	846	15.9	184	
BPIC18	2,514,266	41	43,809	28,457	64.0	2,973	1.61	5.65	1.5	27,279	55.7	1,535	
BPIC19 ₁	5,898	11	1,044	148	10.9	21	0.78	6.02	1.0	109	7.8	15	
BPIC19 ₂	319,233	38	15,182	4,228	60.5	990	1.82	6.67	1.19	3,579	51.6	843	
BPIC19 ₃	1,234,708	39	221,010	7,832	10.5	179	0.14	7.15	1.1	7,404	9.8	63	
BPIC19 ₄	36,084	15	14,498	281	5.7	17	0.23	4.48	1.0	238	5.2	12	
PRT1	75,353	9	12,720	1,026	13.1	64	0.5	4.11	1.55	784	11.6	56	
PRT2	46,282	9	1,182	1,153	39.8	276	1.04	3.96	1.3	1,153	37.2	252	
PRT3	13,720	15	1,600	318	8.6	9	0.0	0.0	0.0	318	8.6	9	
PRT4	166,282	11	20,000	5,941	11.5	36	0.22	3.23	1.03	5,551	11.2	36	
PRT6	6,011	9	744	167	10.1	21	0.01	3.0	2.0	166	10.1	21	
PRT7	16,353	13	2,000	128	9.1	11	0.0	0.0	0.0	128	9.1	11	
PRT9	1,808,706	8	787,657	909	10.5	58	0.4	4.36	1.72	777	8.8	50	
PRT10	78,864	19	43,514	172	3.4	15	0.15	5.42	1.0	151	2.9	8	

Table 1. Logs and reduction statistics

the reachability graph generated from each model (“RG Size”). The complexity of computing alignments is mainly linked to the size of the reachability graph of the process model, which is worst-case exponential on the size of the model. For example, we can observe that the size of the reachability graph of PRT2 (IM) is around 5.5M nodes and arcs, while the corresponding process model has a size of 175 nodes and arcs. In Table 2 we also report the number of S-Components identified per model (“#Scomp”) and the average size of the reachability graph (“ \emptyset RG Size”) after applying the S-Components decomposition (empty cells indicate concurrency-free models – the number of S-Components being 1). We can observe that this size is usually smaller than that of the original reachability graph. For example, for PRT2 (IM) the size is reduced to an average of 15 nodes and arcs. Sometimes, this reduction does not lead to a smaller state space, e.g. for BPIC12 (SM) the size reduces from 95 to 90 per S-Component, which leads to a total state space of 180 nodes and arcs for all S-Components, which is larger than the size of the original model.

The two discovery methods (IM and SM) pose different challenges to conformance checking. Inductive Miner is designed to discover highly-fitting models. As a result, the models often exhibit a larger reachability graph as they need to cater for a large variety of executions present in the logs. Split Miner strikes a trade-off between fitness and precision by filtering the directly-follows graph of the log before discovering the model. The models produced by Split Miner will have a smaller state space but may lead to a higher number of fitness mismatches, and hence to more complex alignments. Altogether, the models obtained by these two methods present two different scenarios for conformance checking: the models discovered by Inductive Miner require a larger state space to be traversed with a low to medium number of mismatches per trace, while the models discovered by Split Miner have a smaller state space with a medium to high number of mismatches per trace.

Miner	Domain	Dataset	Size	Trns	XOR	AND	RG Size	#Scomp	∅ RG Size
IM	public	BPIC12	177	45	16	2	1,997	10	58.3
		BPIC13 _{cp}	31	8	2	0	9	1	
		BPIC13 _{inc}	56	13	3	1	121	3	14.0
		BPIC14 _f	124	29	8	2	4,383	10	26.1
		BPIC15 _{1f}	449	127	48	0	719	1	
		BPIC15 _{2f}	537	150	55	1	1,019	2	232.0
		BPIC15 _{3f}	464	128	47	3	875	8	191.5
		BPIC15 _{4f}	469	131	51	1	1,019	2	202.0
		BPIC15 _{5f}	381	111	31	0	429	1	
		BPIC17 _f	121	33	8	0	59	1	
		RTFMP	111	26	9	2	2,394	6	25.0
		SEPSIS	145	37	13	3	2,274	8	44.0
		BPIC18	235	57	18	6	1,057	72	62.9
		BPIC19 ₁	44	11	4	1	49	2	13.5
	BPIC19 ₂	186	47	13	4	20,264	8	37.3	
	BPIC19 ₃	279	70	23	7	6,450	44	83.4	
	BPIC19 ₄	85	23	8	1	86	2	29.5	
	private	PRT1	70	16	4	1	195	4	19.3
		PRT2	175	43	16	1	5,515,357	7	23.0
		PRT3	111	27	8	2	167	8	33.0
PRT4		91	21	5	2	154	8	26.0	
PRT6		86	20	4	2	65	6	29.0	
PRT7		99	23	5	2	158	8	30.0	
SM	public	PRT9	96	21	7	2	9,121	7	13.9
		PRT10	124	35	8	1	184	2	48.5
		BPIC12	315	85	29	1	95	2	140.0
		BPIC13 _{cp}	49	13	4	0	13	1	
		BPIC13 _{inc}	56	15	5	0	17	1	
		BPIC14 _f	88	24	9	0	24	1	
		BPIC15 _{1f}	368	98	25	0	156	1	
		BPIC15 _{2f}	444	117	25	0	186	1	
		BPIC15 _{3f}	296	78	17	0	136	1	
		BPIC15 _{4f}	323	85	18	0	141	1	
		BPIC15 _{5f}	359	94	18	0	159	1	
		BPIC17 _f	149	40	12	0	54	1	
		RTFMP	102	28	11	0	37	1	
		SEPSIS	162	44	15	0	41	1	
	BPIC18	251	72	16	0	87	1		
	BPIC19 ₁	63	18	4	0	29	1		
	BPIC19 ₂	232	68	14	0	105	1		
	BPIC19 ₃	378	112	20	0	172	1		
	BPIC19 ₄	106	31	8	0	51	1		
	private	PRT1	104	28	9	0	28	1	
PRT2		166	45	15	0	37	1		
PRT3		96	25	8	1	34	2	41.0	
PRT4		126	33	10	1	34	2	55.0	
PRT6		46	11	2	1	20	2	19.0	
PRT7		86	19	3	5	39	6	27.7	
PRT9	107	29	10	0	32	1			
PRT10	327	90	34	0	92	1			

Table 2. Models and S-Components statistics

5.3. Results

In Table 3 we show the time performance in milliseconds (ms) of all approaches against the 50 model-log pairs. The best result for each dataset is highlighted in bold and timeout cases are recorded with “t/out”. The table also shows the number of S-Components (“#SComp”) of the input process model and the average trace reduction length (“ \emptyset Red.”), computed as the average length of the original traces minus the average length of the reduced traces from Table 1. We included these model-log characteristics as they have some explanatory value regarding the time results.

Analyzing the overall performance. The Automata-based approach (Automata) outperforms the other datasets in 32 of 50 cases; its S-Components extension (SComp) performs best in eight out of 50 cases while the use of the tandem repeats reduction on top of the S-Components extension (TR-SComp), performs best in seven out of 50 cases. Both eMEQ and ALI outperform the other approaches in one case only, while the ILP approach never outperforms any other approach. When including the number of times an approach was ranked second, in order to reduce small variations, the results between the Automata-based variants homogenize. The base approach increases to 36 out of 50 cases, the SComp extension increases to 32 of 50 and the TR-SComp variant increases to 27 out of 50. The results of ILP, eMEQ and ALI do not change. When considering the total time spent across all 50 datasets (excluding timed out cases), the TR-SComp approach is the fastest with 251 seconds, followed by the SComp approach at around 300 seconds, the Automata approach at 540 seconds, eMEQ at 840 seconds, ILP at 1,250 seconds and last ALI at 1,600 seconds. The difference between the total execution time (TR-SComp ranks first) and the ranking in individual datasets (TR-SComp ranks third) indicates that the tandem repeats approach reduces execution times significantly but only for certain datasets, i.e. those cases where effectively repetition is observed in the log.

Investigating timeout cases. All approaches time out for dataset BPIC18 when the model discovered is from Inductive Miner. This log has a very high number of unique traces (28,457) and nested parallel structures in the process model, resulting into 72 S-Components. The second most difficult case is PRT2 with Inductive Miner. This log has a very large underlying state space (RG size: 5M), and only ALI can compute alignments. The S-Component approach can compute alignments quickly for most of the traces in this log (the average size of the reachability graph of the S-Components is only 15), though this approach times out when some conflicting traces need to be aligned on the original reachability graph. Our TR-SComp approach is able to compute alignments quickly for other difficult cases (i.e. cases where more than 3 other approaches time out) such as BPIC19₂ (IM) or BPIC18 (SM). In total, the TR-SComp and SComp approaches have the lowest number of timeouts (two cases), followed by ILP and Automata with three, ALI with four and eMEQ with twelve.

Improvements of the tandem repeats approach. The TR-SComp approach outperforms the other approaches significantly when the input event log is reduced on average by at least two events (the average trace reduction length \emptyset Red. is greater than two). For example, in BPIC12 (IM), TR-SComp outperforms S-Components by a factor of two, ALI by five and Automata as well as ILP by an order of magnitude. In the dataset BPIC18 (SM), TR-SComp improves over all the Automata-based variants by 20 seconds, while other approaches could not compute alignments for this model-log pair. In the case of BPIC14_f, TR-SComp outperforms the other approaches even though the average reduction is low (0.4 events per trace). This could be due to the high number of unique traces (circa 15K) such that overall a significant number of events is reduced.

Problematic cases of the tandem repeats approach. Some datasets like the BPIC15 logs do not contain any repeating events. In these cases, TR-SComp performs similarly as the SComp approach, which in turn will fall back to the performance of the Automata-based approach when the process model is concurrency-free (i.e. #SComps=1). In some cases, the log contains a relevant number of repetitions (\emptyset Red.>2), but TR-SComp is not faster than SComp, e.g. in BPIC13_{inc} (IM) or BPIC19₁ (SM). We attribute this to the fact that these model-log pairs are quite small and thus the processing of tandem repeats creates a computational overhead compared to not applying the reduction altogether.

Miner	Dataset	#SComps \varnothing Red.		Baselines					Our technique	
				ILP	eMEQ	ALI	Automata	SComp	TR-SComp	Hybrid
IM	BPIC12	10	14.0	135,911	t/out	49,018	104,523	21,516	11,537	11,537
	BPIC13 _{cp}	1	1.7	123	707	3,836	23	32	38	23
	BPIC13 _{inc}	3	3.8	1,708	59,068	27,850	1,385	137	242	242
	BPIC14 _f	10	0.4	101,837	t/out	100,351	199,488	2,048	11,185	2,048
	BPIC15 _{1f}	1	0.0	3,501	3,041	19,651	126	165	153	126
	BPIC15 _{2f}	2	0.0	20,529	20,759	43,863	1,187	1,739	1,521	1,739
	BPIC15 _{3f}	8	0.0	32,328	60,310	47,525	2,292	4,330	4,118	2,292
	BPIC15 _{4f}	2	0.0	12,184	21,942	33,958	686	1,047	887	1,047
	BPIC15 _{5f}	1	0.0	8,877	11,059	23,239	348	431	427	348
	BPIC17 _f	1	8.6	21,982	167,013	60,621	4,436	4,996	1,314	1,314
	RTFMP	6	0.6	2,449	1,162	5,884	428	674	678	674
	SEPSIS	8	0.4	7,109	17,848	23,842	3,063	1,461	1,590	1,461
	BPIC18	72	8.3	t/out	t/out	t/out	t/out	t/out	t/out	t/out
	BPIC19 ₁	2	3.1	118	542	7,006	38	57	54	54
	BPIC19 ₂	8	9.0	179,802	t/out	t/out	t/out	66,751	61,967	61,967
	BPIC19 ₃	44	0.8	113,305	35,354	71,759	74,565	53,635	54,283	53,635
	BPIC19 ₄	2	0.6	463	676	7,563	52	95	105	95
	PRT1	4	1.5	1,022	1,822	10,812	749	144	255	144
	PRT2	7	2.6	t/out	t/out	17,296	t/out	t/out	t/out	t/out
	PRT3	8	0.0	214	473	6,500	58	84	88	58
PRT4	8	0.3	4,895	7,824	32,811	2,731	486	1,815	2,731	
PRT6	6	0.0	142	347	6,223	33	58	64	33	
PRT7	8	0.0	125	214	5,898	29	71	73	29	
PRT9	7	1.7	34,949	7,763	10,738	21,297	1,890	4,745	1,890	
PRT10	2	0.5	721	564	8,677	37	131	150	131	
SM	BPIC12	2	14.0	199,209	t/out	118,053	6,096	5,783	4,112	6,096
	BPIC13 _{cp}	1	1.7	153	1,609	4,351	22	28	35	22
	BPIC13 _{inc}	1	3.8	1,239	84,507	18,906	210	274	244	244
	BPIC14 _f	1	0.4	41,956	t/out	157,733	10,936	11,498	3,421	10,936
	BPIC15 _{1f}	1	0.0	2,995	1,362	12,986	146	190	196	146
	BPIC15 _{2f}	1	0.0	9,591	5,319	26,114	721	805	869	721
	BPIC15 _{3f}	1	0.0	7,644	8,576	25,067	784	744	755	784
	BPIC15 _{4f}	1	0.0	7,508	5,300	19,893	494	571	568	494
	BPIC15 _{5f}	1	0.0	9,148	4,312	24,608	729	623	658	729
	BPIC17 _f	1	8.6	28,410	53,545	265,169	4,646	5,094	1,306	1,306
	RTFMP	1	0.6	2,421	1,514	7,020	71	374	382	71
	SEPSIS	1	0.4	5,126	t/out	18,821	224	262	243	224
	BPIC18	1	8.3	t/out	t/out	t/out	88,274	96,902	62,026	62,026
	BPIC19 ₁	1	3.1	185	1,136	6,570	35	40	41	41
	BPIC19 ₂	1	9.0	70,222	t/out	t/out	6,497	8,218	8,831	8,831
	BPIC19 ₃	1	0.8	91,644	t/out	104,798	4,136	6,500	4,518	4,136
	BPIC19 ₄	1	0.6	490	1,163	7,501	33	59	67	33
	PRT1	1	1.5	2,243	43,426	10,788	132	271	172	132
	PRT2	1	2.6	39,025	t/out	91,186	910	1,040	1,048	1,048
	PRT3	2	0.0	203	620	6,439	51	93	88	51
PRT4	2	0.3	8,556	129,444	47,776	1,733	1,938	2,432	1,733	
PRT6	2	0.0	83	288	5,997	24	54	59	24	
PRT7	6	0.0	111	209	5,887	25	66	69	25	
PRT9	1	1.7	43,094	82,628	18,165	336	1,194	1,533	336	
PRT10	1	0.5	887	1,363	9,374	48	89	91	48	
Total time spent (ms):				1,256,434	844,811	1,638,124	544,886	304,688	251,052	243,855
Total outperforming:				0	1	1	32	8	7	30
Total first and second:				0	1	1	36	32	27	39
#Timeouts:				3	12	4	3	2	2	2

Table 3. Time performance in milliseconds

Hybrid approach: definition and performance. Since as expected the TR-SComp approach approach improves computation time only for a specific type of input event logs, we decided to define a hybrid approach that only applies the tandem repeat reduction if the traces can be reduced on average by at least two events per trace. In addition, we preserve the hybrid rule from [24], that is, we only apply the S-Component extension if the sum of the reachability graph sizes of all S-Components is not larger than the size of the original reachability graph. If the S-Component extension is not applied to a process model with concurrency, then the tandem repeats reduction is also not applied. We report the results of this Hybrid approach in Table 3. In total, this approach gains eight seconds over TR-SComp, outperforming all other approaches in 32 cases out of 50 and is first- or second-ranked in 39 cases. This is the highest result compared to all other approaches.

Miner	Dataset	Cost						Over-Approximation		
		ILP	eMEQ	ALI	Automata	Scomp	TR-Scomp	Δ ALI	Δ Scomp	Δ TR-Scomp
IM	BPIC15 _{2f}	2.02	2.02	26.73	2.02	2.07	2.07	24.706	0.050	0.050
	SEPSIS	0.12	0.12	12.83	0.12	0.12	0.12	12.714	0.004	0.002
	BPIC19 ₂	0.18	t/out	t/out	t/out	0.18	0.18	t/out	0.001	0.001
	BPIC19 ₃	1.00	1.00	6.56	1.00	1.00	1.01	5.562	0.003	0.008
	PRT6	0.09	0.09	2.31	0.09	0.12	0.12	2.216	0.028	0.028
SM	BPIC12	1.29	t/out	17.87	1.29	1.31	1.31	16.583	0.021	0.020
	BPIC18	t/out	t/out	t/out	7.60	7.60	7.60	t/out	0.000	0.001
	PRT4	1.91	1.91	3.59	1.91	1.91	1.91	1.680	0.000	0.001
	PRT7	1.40	1.40	2.22	1.40	1.40	1.40	0.826	0.003	0.003
	PRT9	0.35	0.35	4.44	0.35	0.35	0.35	4.094	0.000	0.001

Table 4. Cost and over-approximation

Analyzing cost over-approximations. Table 4 shows the cost and over-approximation for all datasets where the TR-SComp approach over-approximates the minimal cost. The table with the cost and over-approximations for all datasets can be found in Appendix B. In total, TR-SComp over-approximates in ten cases out of 50 and computes the minimal cost in all other datasets. In detail, the degree of over-approximation ranges between 0.02% to 2.47% for nine cases and 32% for PRT6 (IM). The over-approximation of the latter dataset may seem high, but the overall fitness of this dataset is very low such that any small variation on the minimal cost will cause a high degree of over-approximation. When drilling down the over-approximation for this model-log pair, we found that the cost was on average higher than the minimal by 1.05 in 2.7% of the unique traces. In comparison, ALI, as a representative approach for approximate alignment computation, over-approximates the minimal cost in all datasets ranging from 17% to eleven times the value of the optimal cost. More specifically, ALI over-approximates the optimal cost by more than 100% in 38 cases out of 50. Both TR-SComp and ALI never under-estimate the optimal cost by construction.

Investigating causes of over-approximation. The first reason for over-approximation is that the TR-SComp approach is applied on top of the SComp approach and as such it carries the over-approximation induced by this latter approach [24]. Specifically, the cost will be over-approximated if a trace contains an activity that is after a parallel block in the process model, but appears before the activities of the parallel block in the trace, i.e. it is misplaced. This was the most common cause of over-approximation.

As a second reason, TR-SComp induces over-approximation when a tandem repeat involves exactly three repetitions and no repeating sequence can be found in the returned reduced alignment of Alg. 2. The over-approximation occurs if there exists another reduced alignment with the same cost that could contain a repeating sequence. In that case, the extended alignment would include a middle copy of the tandem repeat with all *LH*-operations while some of the events could actually be matched. We encountered this problem for example in the dataset PRT4 (SM). The snippet of the problematic part of the process model is shown in Fig. 9. Here an activity “Background at Rugby Run” can be repeated any number of times and is then followed by activity “Background at Croyden”, which can also be repeated.

The problematic tandem repeat is (2, Background at Croyden, Background at Rugby Run), 3), i.e. the repeat type “Background at Croyden, Background at Rugby Run” is repeated three times at the trace position

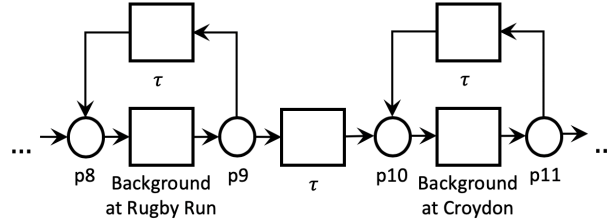


Figure 9. Snippet of the process model PRT4 (SM), where an over-approximation occurs

two. The reduced tandem repeat containing only two copies is then aligned with $\langle (LH, \text{Background at Croyden}), (MT, \text{Background at Rugby Run}), (MT, \text{Background at Croyden}), (LH, \text{Background at Rugby Run}) \rangle$. When trying to extend this tandem repeat with Alg. 3, we can not identify a repeating sequence within this tandem repeat since neither of the two activities has been aligned with a MT in both copies of the tandem repeat. Hence, the extended alignment would include both activities with LH operations and incur a cost of two. However, there exists another alignment for the reduced tandem repeat with the same cost, where a repeating sequence can be found, i.e. $\langle (LH, \text{Background at Croyden}), (MT, \text{Background at Rugby Run}), (LH, \text{Background at Croyden}), (MT, \text{Background at Rugby Run}), (RH, \text{Background at Croyden}) \rangle$. For that alignment activity “Background at Rugby Run” can now be identified as a repeating sequence and will be included with a MT operation in the middle copy such that only a cost of one is added. The problem of over-approximation occurs because we find the former alignment and not the latter since they have the same cost and we only find one optimal alignment with Alg. 2.

The reason why the two alignments have the same cost is that the two activities in the trace are reversed in the order of the process model such that only one activity can be repeated and the other needs to be hidden in both the trace and the model, or both activities can be matched and then no repetitions can be matched resulting in an overall cost of four in both cases. We observe that this situation cannot happen for higher numbers of repetitions since the alignment that matches the two activities without any repetitions incurs an additional cost from the collapsed repetitions. Specifically, the former alignment would have a cost of six while the latter alignment would have a cost of five. Thus, the correct alignment would be returned by Alg. 2, avoiding the over-approximation.

To avoid such cases of over-approximation, it would be possible to discard tandem repeats of three repetitions during the reduction, in order to increase the precision of the tandem repeats approach. However, the amount of over-approximation caused by this issue was rather low in the evaluated datasets and thus we argue that trading a small amount of accuracy for potential gains in performance is worthwhile.

5.4. Threats to validity

The selection of datasets constitutes a threat to validity. We decided to use two datasets of real-life log-model pairs from a recent discovery benchmark [40], and enriched this with the BPIC logs from the last two years to keep the dataset up to date. These model-log pairs exhibit a wide range of structural characteristics and originate from different industry domains, so they provide a good representation of reality. However, some of the event logs such as the whole BPIC15 series do not contain any repeating events. This calls for further experiments with event logs with a higher degree of repetitions, and more in general, with very large real-life log-model pairs. Such datasets are not publicly available at the time of writing. This problem could be alleviated by the use artificial datasets as in [54].

The selection of the baseline approaches is another threat to validity. The technique proposed in this article, as well as the Automata-based technique and its S-Components extension, are applicable to a specific subclass of Petri nets, namely 1-safe sound workflow nets, while the two exact approaches chosen as baselines (ILP and eMEQ) are applicable to a wider class of Petri nets, namely easy sound Petri nets, and the approximate technique (ALI) is applicable to sound Petri nets. To the best of our knowledge, however, there are no conformance checking techniques available that target the specific subclass of Petri

nets addressed by our technique for a better comparison. In addition, this specific class of Petri nets has relevance to the the field of process mining and more widely to the field of business process management, since BPMN models can be translated to this class and several mining algorithms such as Split Miner [51], Inductive Miner [50] or Fodina [53] produce Petri nets of this class.

A final threat to validity is posed by the number of methods used for automated process discovery (only two). Potentially we could have chosen a larger number of methods. The choice of Split Miner and Inductive Miner was determined by both pragmatic reasons (other methods such as Structured Heuristics Miner return models with duplicate events which we cannot handle, or lead to models for which fitness could not be computed) as well as by the need to test two extreme cases: models with large state spaces versus event logs with large degrees of repeated activities. Moreover, they are the best performing automated discovery methods according to the benchmark in [40]. So, all considered, they constitute a sufficiently representative set of automated discovery methods.

6. Conclusion

This article contributes a technique for the efficient computation of alignments in the field of conformance checking. The technique revolves around two key optimizations. First, we show how to use a specific type of repeat pattern, namely tandem repeats, to reduce an event log by collapsing repetitive behavior. We compute alignments on this reduced log and later extend these alignments to work on the original event log. We prove that these two operations (reduction and later expansion) lead to proper alignments in the original log, in the context of concurrency-free process models. While this first optimization helps us reduce the computation time of each alignment in the presence of repeated behavior in the log, as a second optimization, we use a binary search to identify reduced traces that map to the same unique trace in the original log. This allows us to reduce the overall number of alignments to be computed, hence further improving the computation time.

The proposed technique is applicable to concurrency-free process models. However, we show how the technique can be integrated in a decomposition framework to also work in the context of models that exhibit concurrency. In this article, we propose the use of the S-Component decomposition [24] since it naturally outputs concurrency free process models. However, the technique is not specifically tight to this particular decomposition approach, i.e. other decomposition approaches may be used so long as they produce concurrency-free process models.

Our technique builds on top of our previous approach for Automata-based alignments computation [10, 24]. However, the optimizations proposed by this technique are independent from the selected approach and could also be used in conjunction with other trace alignment approaches, e.g. those approaches that align one trace at a time, such as [37] and [4]. Adapting the technique to work on top of these approaches is an avenue for future work.

In an extensive evaluation using 50 real-life model-log pairs, we showed that our technique used on top of the Automata-based approach systematically outperforms five baseline approaches, in the presence of significant repetitive behavior in the log. We also showed that the cost over-approximation induced by our technique, when it occurs, is negligible. To benefit from the reduction only when this is really needed, and avoid applying it when not needed, we presented a hybrid approach that selects which extension to the Automata-based conformance checking approach should be applied, based on characteristics of the input log and model. We derived these criteria empirically based on the evaluation results. More research could be conducted on finding finer-grained rules for applying our technique based on more specific model-log characteristics.

This article addressed the problem of identifying unfitting log behavior. However, the ideas investigated here could also be applied to the related problem of identifying how well model structures generalize patterns of an event log [12]. This latter problem is related to that of measuring the precision of a process model relative to an event log, which is an open problem in the field of process mining [55]. Another avenue for future work is to investigate the application of tandem repeats to the problem of identifying and measuring additional process model behavior that generalizes the behavior in the log.

Acknowledgments. This research is partly funded by the Australian Research Council (grant DP180102839).

References

- [1] M. Dumas, M. La Rosa, J. Mendling, H. Reijers, *Fundamentals of Business Process Management*, Vol. 2nd Edition, Springer, 2018.
- [2] W. van der Aalst, *Process Mining - Data Science in Action*, Second Edition, Springer, 2016.
- [3] A. Adriansyah, B. van Dongen, W. van der Aalst, Conformance checking using cost-based fitness analysis, in: *Proc. of EDOC, IEEE*, 2011, pp. 55–64.
- [4] B. van Dongen, Efficiently computing alignments: using the extended marking equation, in: M. Montali, I. Weber, M. Weske, J. vom Brocke (Eds.), *Business Process Management - 16th International Conference, BPM 2018, Proceedings, Lecture Notes in Computer Science (including subseries Lecture Notes in Artificial Intelligence and Lecture Notes in Bioinformatics)*, Springer, Germany, 2018, pp. 197–214.
- [5] B. van Dongen, F. Borchert, Bpi challenge 2018 (2018). doi:10.4121/UUID:3301445f-95e8-4ff0-98a4-901f1f204972. URL <https://data.4tu.nl/repository/uuid:3301445f-95e8-4ff0-98a4-901f1f204972>
- [6] A. Augusto, R. Conforti, M. Dumas, M. La Rosa, F. Maggi, A. Marrella, M. Mecella, A. Soo, Automated discovery of process models from event logs: Review and benchmark, *IEEE Trans. Knowl. Data Eng.* 31 (4) (2019) 686–705.
- [7] D. Gusfield, J. Stoye, Linear time algorithms for finding and representing all the tandem repeats in a string, *Journal of Computer and System Sciences* 69 (4) (2004) 525 – 546. doi:<https://doi.org/10.1016/j.jcss.2004.03.004>. URL <http://www.sciencedirect.com/science/article/pii/S0022000004000364>
- [8] R. Bose, W. van der Aalst, Abstractions in process mining: A taxonomy of patterns, in: *Business Process Management*, 2009, pp. 159–175.
- [9] A. Adriansyah, *Aligning observed and modeled behavior*, Ph.D. thesis, TU/e (2014).
- [10] D. Reißner, R. Conforti, M. Dumas, M. La Rosa, A. Armas-Cervantes, Scalable conformance checking of business processes, in: H. Panetto, C. Debruyne, W. Gaaloul, M. Papazoglou, A. Paschke, C. Ardagna, R. Meersman (Eds.), *On the Move to Meaningful Internet Systems. OTM 2017 Conferences*, Springer International Publishing, Cham, 2017, pp. 607–627.
- [11] M. de Leoni, A. Marrella, Aligning real process executions and prescriptive process models through automated planning, *Expert Systems with Applications* 82 (2017) 162–183.
- [12] L. García-Bañuelos, N. van Beest, M. Dumas, M. La Rosa, W. Mertens, Complete and interpretable conformance checking of business processes, *IEEE Transactions on Software Engineering* 44 (3) (2018) 262–290.
- [13] M. Nielsen, G. Plotkin, G. Winskel, Petri nets, event structures and domains, part I, *Theoretical Computer Science* 13 (1).
- [14] B. van Dongen, J. Carmona, T. Chatain, F. Taymouri, Aligning modeled and observed behavior: a compromise between complexity and quality, in: *Proc. of CAiSE*, Springer, 2017.
- [15] F. Taymouri, J. Carmona, Computing alignments of well-formed process models using local search, *ACM Transactions on Software Engineering and Methodology* (2020) Preprint available at <http://hdl.handle.net/11343/234396>.
- [16] F. Taymouri, J. Carmona, An evolutionary technique to approximate multiple optimal alignments, in: M. Weske, M. Montali, I. Weber, J. vom Brocke (Eds.), *Business Process Management*, Springer International Publishing, Cham, 2018, pp. 215–232.
- [17] M. Bauer, H. van der Aa, M. Weidlich, Estimating process conformance by trace sampling and result approximation, in: T. Hildebrandt, B. van Dongen, M. Röglinger, J. Mendling (Eds.), *Business Process Management*, Springer International Publishing, Cham, 2019, pp. 179–197.
- [18] A. Burattin, S. van Zelst, A. Armas-Cervantes, B. van Dongen, J. Carmona, Online conformance checking using behavioural patterns, in: M. Weske, M. Montali, I. Weber, J. vom Brocke (Eds.), *Business Process Management*, Springer International Publishing, Cham, 2018, pp. 250–267.
- [19] W. van der Aalst, Decomposing petri nets for process mining: A generic approach, *Distributed and Parallel Databases* 31 (4) (2013) 471–507.
- [20] J. Muñoz-Gama, J. Carmona, W. van der Aalst, Single-entry single-exit decomposed conformance checking, *Inf. Syst.* 46 (2014) 102–122.
- [21] L. Wang, Y. Du, W. Liu, Aligning observed and modelled behaviour based on workflow decomposition, *Enterprise Information Systems* 11 (8) (2017) 1207–1227.
- [22] H. Verbeek, W. van der Aalst, Merging alignments for decomposed replay, in: *International Conference on Application and Theory of Petri Nets and Concurrency*, Springer, 2016, pp. 219–239.
- [23] W. Song, X. Xia, H. Jacobsen, P. Zhang, H. Hu, Efficient alignment between event logs and process models, *IEEE Transactions on Services Computing* 10 (1) (2017) 136–149.
- [24] D. Reißner, A. Armas-Cervantes, R. Conforti, M. Dumas, D. Fahland, M. La Rosa, Scalable alignment of process models and event logs: An approach based on automata and s-components, *Tech. Rep. 1910.09767*, arXiv.org (2019, <https://arxiv.org/abs/1910.09767>).
- [25] S. Shanmugasundaram, R. Lourdasamy, A comparative study of text compression algorithms, *International Journal of Wisdom Based Computing* 1 (3) (2011) 68–76.
- [26] J. Ziv, A. Lempel, A universal algorithm for sequential data compression, *IEEE Transactions on information theory* 23 (3) (1977) 337–343.
- [27] J. Ziv, A. Lempel, Compression of individual sequences via variable-rate coding, *IEEE transactions on Information Theory* 24 (5) (1978) 530–536.

- [28] J. A. Storer, T. G. Szymanski, Data compression via textual substitution, *Journal of the ACM (JACM)* 29 (4) (1982) 928–951.
- [29] T. Welch, A technique for high-performance data compression, *Computer* (6) (1984) 8–19.
- [30] E. Fiala, D. Greene, Data compression with finite windows, *Communications of the ACM* 32 (4) (1989) 490–505.
- [31] G. Sirisha, M. Shashi, G. Raju, Periodic pattern mining—algorithms and applications, *Global Journal of Computer Science and Technology*.
- [32] W. van der Aalst, The application of petri nets to workflow management, *Journal of Circuits, Systems and Computers* 08 (01) (1998) 21–66.
- [33] J. Desel, J. Esparza, *Free choice Petri nets*, Vol. 40, Cambridge university press, 2005.
- [34] H. Verbeek, T. Basten, W. van der Aalst, Diagnosing Workflow Processes using Woflan, *Comput. J.* 44 (4) (2001) 246–279.
- [35] E. Mayr, An algorithm for the general petri net reachability problem, *SIAM journal on computing* 13 (3) (1984) 441–460.
- [36] R. Lipton, The reachability problem requires exponential space, Research Report 62, Department of Computer Science, Yale University, New Haven, Connecticut.
- [37] A. Adriansyah, B. van Dongen, W. van der Aalst, Conformance checking using cost-based fitness analysis, in: 2011 IEEE 15th International Enterprise Distributed Object Computing Conference, 2011, pp. 55–64.
- [38] M. Abouelhoda, S. Kurtz, E. Ohlebusch, Replacing suffix trees with enhanced suffix arrays, *Journal of Discrete Algorithms* 2 (1) (2004) 53 – 86.
- [39] M. La Rosa, H. Reijers, W. van der Aalst, R. Dijkman, J. Mendling, M. Dumas, L. García-Bañuelos, APROMORE: an advanced process model repository, *Expert Syst. Appl.* 38 (6) (2011) 7029–7040. doi:10.1016/j.eswa.2010.12.012. URL <https://doi.org/10.1016/j.eswa.2010.12.012>
- [40] A. Augusto, R. Conforti, M. Dumas, M. La Rosa, F. Maggi, A. Marrella, M. Mecella, A. Soo, Automated discovery of process models from event logs: Review and benchmark, *IEEE Transactions on Knowledge and Data Engineering* 31 (4) (2019) 686–705.
- [41] B. van Dongen, Bpi challenge 2012 (2012). doi:10.4121/UUID:3926DB30-F712-4394-AEBC-75976070E91F. URL <https://data.4tu.nl/repository/uuid:3926db30-f712-4394-aebc-75976070e91f>
- [42] W. Steeman, Bpi challenge 2013, closed problems (2013). doi:10.4121/UUID:C2C3B154-AB26-4B31-A0E8-8F2350DDAC11. URL <https://data.4tu.nl/repository/uuid:c2c3b154-ab26-4b31-a0e8-8f2350ddac11>
- [43] W. Steeman, Bpi challenge 2013, incidents (2013). doi:10.4121/UUID:500573E6-ACCC-4B0C-9576-AA5468B10CEE. URL <https://data.4tu.nl/repository/uuid:500573e6-acc-4b0c-9576-aa5468b10cee>
- [44] B. van Dongen, Bpi challenge 2014 (2014). doi:10.4121/UUID:C3E5D162-0CFD-4BB0-BD82-AF5268819C35. URL <https://data.4tu.nl/repository/uuid:c3e5d162-0cfd-4bb0-bd82-af5268819c35>
- [45] B. van Dongen, Bpi challenge 2015 (2015). doi:10.4121/UUID:31A308EF-C844-48DA-948C-305D167A0EC1. URL <https://data.4tu.nl/repository/uuid:31a308ef-c844-48da-948c-305d167a0ec1>
- [46] B. van Dongen, Bpi challenge 2017 (2017). doi:10.4121/UUID:5F3067DF-F10B-45DA-B98B-86AE4C7A310B. URL <https://data.4tu.nl/repository/uuid:5f3067df-f10b-45da-b98b-86ae4c7a310b>
- [47] M. de Leoni, F. Mannhardt, Road traffic fine management process (2015). doi:10.4121/UUID:270FD440-1057-4FB9-89A9-B699B47990F5. URL <https://data.4tu.nl/repository/uuid:270fd440-1057-4fb9-89a9-b699b47990f5>
- [48] F. Mannhardt, Sepsis cases - event log (2016). doi:10.4121/UUID:915D2BFB-7E84-49AD-A286-DC35F063A460. URL <https://data.4tu.nl/repository/uuid:915d2bfb-7e84-49ad-a286-dc35f063a460>
- [49] R. Conforti, M. La Rosa, A. Ter Hofstede, Filtering out infrequent behavior from business process event logs, *IEEE Transactions on Knowledge and Data Engineering* 29 (2) (2016) 300–314.
- [50] S. Leemans, D. Fahland, W. van der Aalst, Discovering block-structured process models from event logs—a constructive approach, in: *International conference on applications and theory of Petri nets and concurrency*, Springer, 2013, pp. 311–329.
- [51] A. Augusto, R. Conforti, M. Dumas, M. La Rosa, Split miner: Discovering accurate and simple business process models from event logs, in: 2017 IEEE International Conference on Data Mining (ICDM), IEEE, 2017, pp. 1–10.
- [52] A. Augusto, R. Conforti, M. Dumas, M. L. Rosa, G. Bruno, Automated discovery of structured process models from event logs: The discover-and-structure approach, *Data Knowl. Eng.* 117 (2018) 373–392.
- [53] S. vanden Broucke, J. De Weerd, Fodina: A robust and flexible heuristic process discovery technique, *Decision Support Systems* 100 (2017) 109 – 118, *smart Business Process Management*.
- [54] J. Muñoz-Gama, Conformance checking in the large (dataset) (2013). doi:10.4121/UUID:44C32783-15D0-4DBD-AF8A-78B97BE3DE49. URL <https://data.4tu.nl/repository/uuid:44c32783-15d0-4dbd-af8a-78b97be3de49>
- [55] N. Tax, X. Lu, N. Sidorova, D. Fahland, W. M. P. van der Aalst, The imprecisions of precision measures in process mining, *Inf. Process. Lett.* 135 (2018) 1–8. doi:10.1016/j.ipl.2018.01.013. URL <https://doi.org/10.1016/j.ipl.2018.01.013>

Appendix A. Extended Alignments are Proper Alignments

Lemma Appendix A.1 (An extended alignment is a proper alignment). *Given a trace $t \in L$, the alignment ϵ_{ext} , returned by Alg. 3, is a proper alignment. Thus, the following two properties hold for ϵ_{ext} :*

1. *the labels in the synchronizations related to the DAFSA represent the trace, i.e. $\lambda(\epsilon|_D(\epsilon_{ext})) = t$, and*
2. *the arcs in the synchronizations related to the reachability graph forms a path through the reachability graph, i.e., for $path = a_{RG}(\epsilon|_{RG}(\epsilon_{ext}))$ holds $src(path(1)) = s_{RG} \wedge tgt(path(|path|)) \in R_{RG} \wedge \forall i \in 1..|path| - 1 : tgt(path(i)) = src(path(i + 1))$.*

For the proof of lemma 4.1, the extended alignment ϵ_{ext} are related to the reduced alignment ϵ linked with trace t via its reduced trace, i.e. $\epsilon = \mathcal{A}(Reductions(t)) = (rt, p, k_{red}, TR_l)$. It has been shown in [24] that the reduced alignment ϵ represents the trace labels of the reduced trace rt as well as forms a path through the reachability graph.

The difference between t and rt is recorded in functions TR_c and p in Alg. 1 as every tandem repeat starting at position $i \in dom(TR_c)$ is reduced to only two copies present in rt . These two copies are aligned in ϵ with two subsequences of the alignment ϵ_1 and ϵ_2 acc. to Def 4.3. The additional cost function p then links each tandem repeat to the amount of reduced repetitions.

In Alg. 3, we insert a sequence of synchronizations ϵ_{mid} after the first aligned copy of each tandem repeat, i.e. after ϵ_1 , for k -amount of times. Thus for proving the two properties of lemma 4.1, we only need to investigate, if sequence ϵ_{mid} adds the same trace labels as the tandem repeat type, i.e. if $\lambda(\epsilon|_D(\epsilon_{mid})) = rt(i..TR_c(i) - 1)$, and if the added arcs of the reachability graph form a valid path.

The construction of ϵ_{mid} depends on whether the aligned two copies of the tandem repeat in ϵ contains a trace label of both copies that is aligned with a MT synchronization ($j > 0$ in Def. 4.3). If such a subsequence is found, we create the middle copy as all synchronizations from the start of the second copy to the position of the matched label, adding all synchronizations after the position of the matched label in the first copy up to the end of the first copy. If no label of the tandem repeat can be matched in both copies, ϵ_{mid} consists of all LH -synchronizations for each trace label in the sequence of the first tandem repeat.

Proof Appendix A.1. *We can now prove the two properties of Lemma 4.1 below:*

1. *Property 1 holds by construction. The extended alignment ϵ_{ext} adds all synchronizations from the reduced alignment ϵ as shown in line 6 thus it holds that $\lambda(a_D(\epsilon_{ext})) = rt$. In addition, Alg. 3 applies the extension defined in Def. 4.3 by adding $p(i)$ times a middle copy for each last position i of a tandem repeat. This reconstructs the original trace t iff the trace labels of the middle copy equals the labels of the tandem repeat. If no repeating subsequence is found, this is trivially true since ϵ_{mid} is constructed of all LH -synchronizations for the first aligned copy ϵ_1 of the tandem repeat, which corresponds to the trace labels of the tandem repeat. In case a repeatable subsequence exists beginning at j as defined in Def. 4.3, ϵ_{mid} consists of the prefix of the second copy ϵ_2 up to index $TR_c(\epsilon, j)$ and then adds the suffix of the first copy after j . It holds that $\lambda(\epsilon|_D(\epsilon_1)) = \lambda(\epsilon|_D(\epsilon_2)) = rt(TR_c(i) - 1..i)$ since both copies of the tandem repeat contain the same labels. The constructed middle copy from Def. 4.3 then contains all trace labels of the tandem repeat since it adds the prefix of the trace labels of the second copy and the suffix of the trace labels of the first copy of the same position of the repeat type of the tandem repeat, i.e. $TR_c(\epsilon, j)$ and j respectively.*
2. *We will prove that property 2 holds, i.e. that the insertion of a middle copy is still a path in the reachability graph. The general case will follow by induction. First, note that a reduced alignment forms a path in the reachability graph.*

Alg. 3 applies the extension defined in Def. 4.3 by adding $p(i)$ times a middle copy for each last position i of a tandem repeat. We now need to show that after adding this middle copy ϵ_{mid} that $a_{RG}(\epsilon|_{RG}(\epsilon_{ext}))$ again forms a path through the reachability graph.

In the case that no repeating subsequence is found, this is trivially true since ϵ_{mid} is constructed of all LH -synchronizations for the first aligned copy of the tandem repeat. It follows that no new arcs in the reachability graph are added to ϵ_{ext} and the path of ϵ is not changed.

In the case of a repeatable subsequence at a position j , ϵ_{mid} consists of the prefix of the second copy up to index $TR_c(\epsilon, j)$ and then adds the suffix of the first copy after j . Take the last element in the synchronizations of the first copy of the tandem repeat, the first element in the middle copy (as defined in Def. 4.3) is the same as the initial element of the second copy, thus its insertion is also a path in the reachability graph for the first element. All elements until and including $TR_c(\epsilon, j)$ will also form a path since they are equal to the synchronizations of the second copy. The next element being inserted is in the first copy at position $j + 1$. From Def. 4.3, we know that both MT-synchronizations for the same label. Since in this work we only consider uniquely-labelled workflow nets, it follows that both MT-synchronizations at $\epsilon[j]$ and $\epsilon[TR_c(\epsilon, j)]$ relate to the same transition and thus the arcs of the reachability graph in between the two matches form a loop. Hence, inserting the element of the first copy at position $j+1$ will form a path since it has the same execution state of the process model after the synchronization at position j . All remaining elements of the middle copy after $j+1$ form a path since they are equal to the suffix of ϵ_1 . In the case that only one copy is inserted the proof is complete since the last element of the middle copy is equal to the last element in the first copy which then forms a path to the first element of the second copy. In case multiple middle copies are inserted, the last element of the middle copy also needs to form a path to its first element. This holds, because the first element of the middle copy is the same as the first element in the second copy and the last element of the middle copy is the last element of the first copy, which also form a path in the reduced alignment. It follows that inserting any number of repetitions of the middle copy as per Def. 4.3 will again form a path through the reachability graph. This holds especially for Petri nets that are parallelism free.

Appendix B. Complete cost comparison and order of approximation

Miner	Dataset	Cost						Over-Approximation		
		ILP	eMEQ	ALI	Automata	Scomp	TR-Scomp	Δ ALI	Δ Scomp	Δ TR-Scomp
IM	BPIC12	0.87	t/out	3.38	0.87	0.87	0.87	2.51	0.00	0.00
	BPIC13 _{cp}	1.46	1.46	2.36	1.46	1.46	1.46	0.89	0.00	0.00
	BPIC13 _{inc}	0.84	0.84	4.14	0.84	0.84	0.84	3.31	0.00	0.00
	BPIC14 _f	1.94	0.00	3.58	1.94	1.94	1.94	1.65	0.00	0.00
	BPIC15 _{1f}	0.50	0.50	15.01	0.50	0.50	0.50	14.51	0.00	0.00
	BPIC15 _{2f}	2.02	2.02	26.73	2.02	2.07	2.07	24.71	0.05	0.05
	BPIC15 _{3f}	1.70	1.70	25.67	1.70	1.70	1.70	23.97	0.00	0.00
	BPIC15 _{4f}	1.14	1.14	22.84	1.14	1.14	1.14	21.71	0.00	0.00
	BPIC15 _{5f}	1.20	1.20	24.90	1.20	1.20	1.20	23.70	0.00	0.00
	BPIC17 _f	0.83	0.83	11.53	0.83	0.83	0.83	10.70	0.00	0.00
	RTFMP	0.06	0.06	2.19	0.06	0.06	0.06	2.13	0.00	0.00
	SEPSIS	0.12	0.12	12.83	0.12	0.12	0.12	12.71	0.00	0.00
	BPIC18	0.00	t/out	t/out	0.00	t/out	0.00	t/out	t/out	0.00
	BPIC19 ₁	0.30	0.30	3.13	0.30	0.30	0.30	2.83	0.00	0.00
	BPIC19 ₂	0.18	t/out	t/out	t/out	0.18	0.18	t/out	0.00	0.00
	BPIC19 ₃	1.00	1.00	6.56	1.00	1.00	1.01	5.56	0.00	0.01
	BPIC19 ₄	0.27	0.27	3.12	0.27	0.27	0.27	2.85	0.00	0.00
	PRT1	1.43	1.43	4.42	1.43	1.43	1.43	3.00	0.00	0.00
	PRT2	0.00	t/out	38.16	0.00	0.00	0.00	38.16	0.00	0.00
	PRT3	0.23	0.23	3.84	0.23	0.23	0.23	3.61	0.00	0.00
PRT4	1.22	1.22	4.79	1.22	1.22	1.22	3.56	0.00	0.00	
PRT6	0.09	0.09	2.31	0.09	0.12	0.12	2.22	0.03	0.03	
PRT7	0.00	0.00	2.10	0.00	0.00	0.00	2.10	0.00	0.00	
PRT9	0.38	0.38	3.09	0.38	0.41	0.38	2.71	0.03	0.00	
PRT10	0.06	0.06	3.16	0.06	0.06	0.06	3.10	0.00	0.00	
SM	BPIC12	1.29	t/out	17.87	1.29	1.31	1.31	16.58	0.02	0.02
	BPIC13 _{cp}	0.09	0.09	2.19	0.09	0.09	0.09	2.10	0.00	0.00
	BPIC13 _{inc}	0.24	0.24	3.77	0.24	0.24	0.24	3.54	0.00	0.00
	BPIC14 _f	2.91	t/out	5.83	2.91	2.91	2.91	2.92	0.00	0.00
	BPIC15 _{1f}	3.20	3.20	19.38	3.20	3.20	3.20	16.18	0.00	0.00
	BPIC15 _{2f}	10.22	10.22	27.44	10.22	10.22	10.22	17.21	0.00	0.00
	BPIC15 _{3f}	9.70	9.70	13.75	9.70	9.70	9.70	4.06	0.00	0.00
	BPIC15 _{4f}	10.42	10.42	22.23	10.42	10.42	10.42	11.81	0.00	0.00
	BPIC15 _{5f}	8.10	8.10	17.04	8.10	8.10	8.10	8.94	0.00	0.00
	BPIC17 _f	1.47	1.47	18.94	1.47	1.47	1.47	17.47	0.00	0.00
	RTFMP	0.03	0.03	2.77	0.03	0.03	0.03	2.73	0.00	0.00
	SEPSIS	4.72	t/out	12.23	4.72	4.72	4.72	7.51	0.00	0.00
	BPIC18	t/out	t/out	t/out	7.60	7.60	7.60	t/out	0.00	0.00
	BPIC19 ₁	0.65	0.65	3.23	0.65	0.65	0.65	2.58	0.00	0.00
	BPIC19 ₂	1.02	t/out	t/out	1.02	1.02	1.02	t/out	0.00	0.00
	BPIC19 ₃	0.09	t/out	7.64	0.09	0.09	0.09	7.55	0.00	0.00
	BPIC19 ₄	0.03	0.03	2.56	0.03	0.03	0.03	2.53	0.00	0.00
	PRT1	0.29	0.29	4.13	0.29	0.29	0.29	3.83	0.00	0.00
	PRT2	8.32	t/out	34.53	8.32	8.32	8.32	26.22	0.00	0.00
	PRT3	2.54	2.54	6.50	2.54	2.54	2.54	3.96	0.00	0.00
PRT4	1.91	1.91	3.59	1.91	1.91	1.91	1.68	0.00	0.01	
PRT6	1.08	1.08	1.26	1.08	1.08	1.08	0.19	0.00	0.00	
PRT7	1.40	1.40	2.22	1.40	1.40	1.40	0.83	0.00	0.00	
PRT9	0.35	0.35	4.44	0.35	0.35	0.35	4.09	0.00	0.01	
PRT10	0.10	0.10	3.08	0.10	0.10	0.10	2.98	0.00	0.00	

Table B.5. Full cost comparison